HYPERCOMP
Hyperspectral Computing Laboratory

Departamento de Tecnología de Computadores y Comunicaciones
Department of Technologies of Computers and Communications
Universidad de Extremadura. Escuela Politécnica, 10003 Cáceres, España (Spain) tcc.unex.es

Ph.D. Thesis:

New Probabilistic Classification Techniques for Hyperspectral Images

Author: Mahdi Khodadadzadeh
Advisors: Antonio Plaza Miguel
Jun Li

Outline

Introduction

Proposed Methods

Pixelwise Hyperspectral Classification

Combining local and global probabilities

Subspace-based MLR algorithm based on class-indexed subspaces

Subspace-based MLR algorithm based on union of subspaces

Spectral-Spatial Hyperspectral Classification

Discontinuity preserving relaxation

Fusion of Hyperspectral and LiDAR data

Conclusions and future research lines

Introduction

- Hyperspectral image classification
- Integration of spatial and spectral information
- Subsapce-based methods
- Data set

Hyperspectral image

- Hyperspectral sensors provide rich spectral information for distinguishing different land cover types such as water, soil and vegetation.

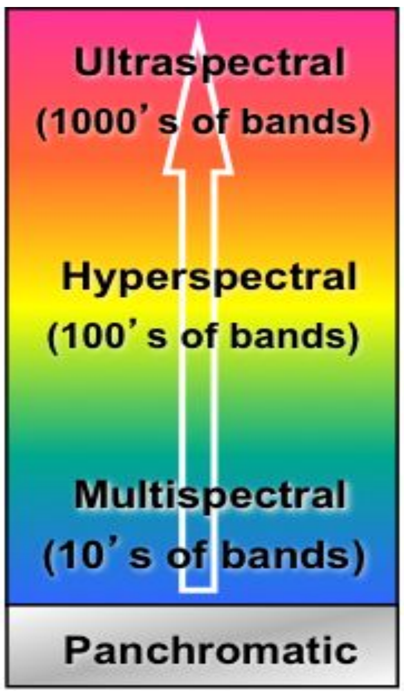

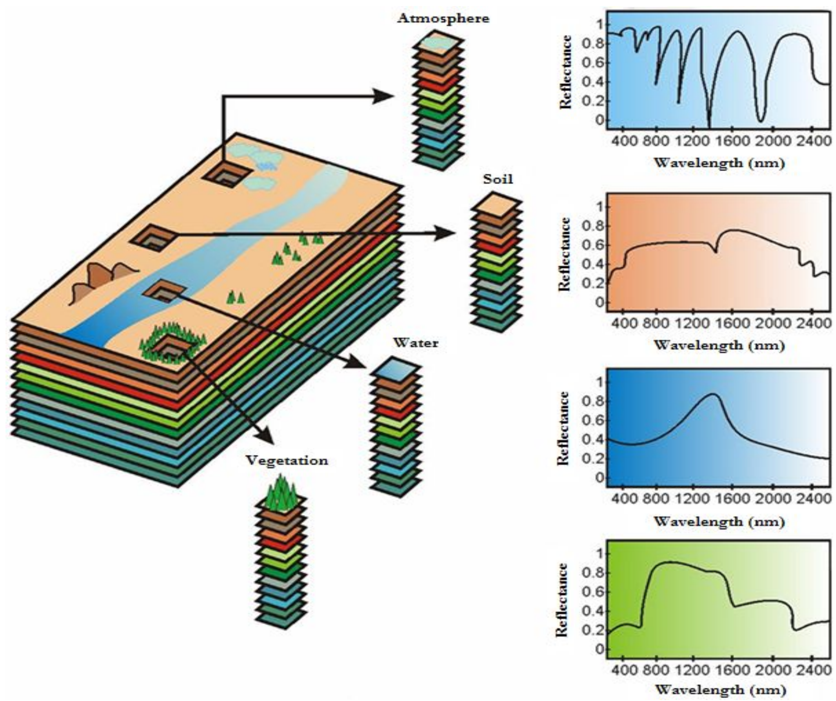

Classification problem

- Given a set of observations (i.e., pixel vectors in a hyperspectral image), the goal of classification is to assign a distinct class label to every pixel in the image.

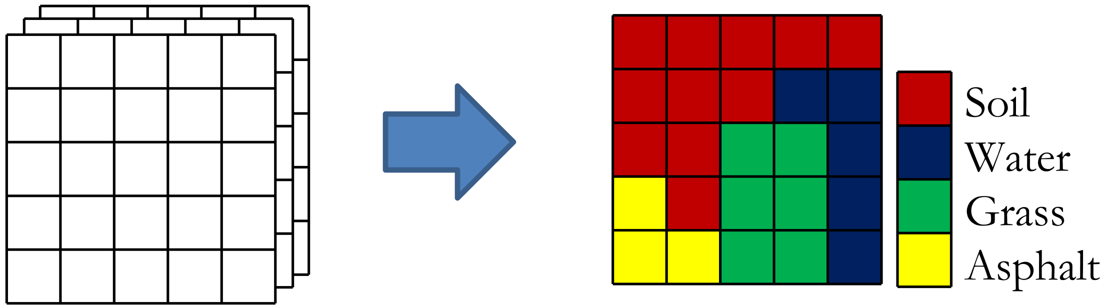

Classification problem

- Given a set of observations (i.e., pixel vectors in a hyperspectral image), the goal of classification is to assign a distinct class label to every pixel in the image.

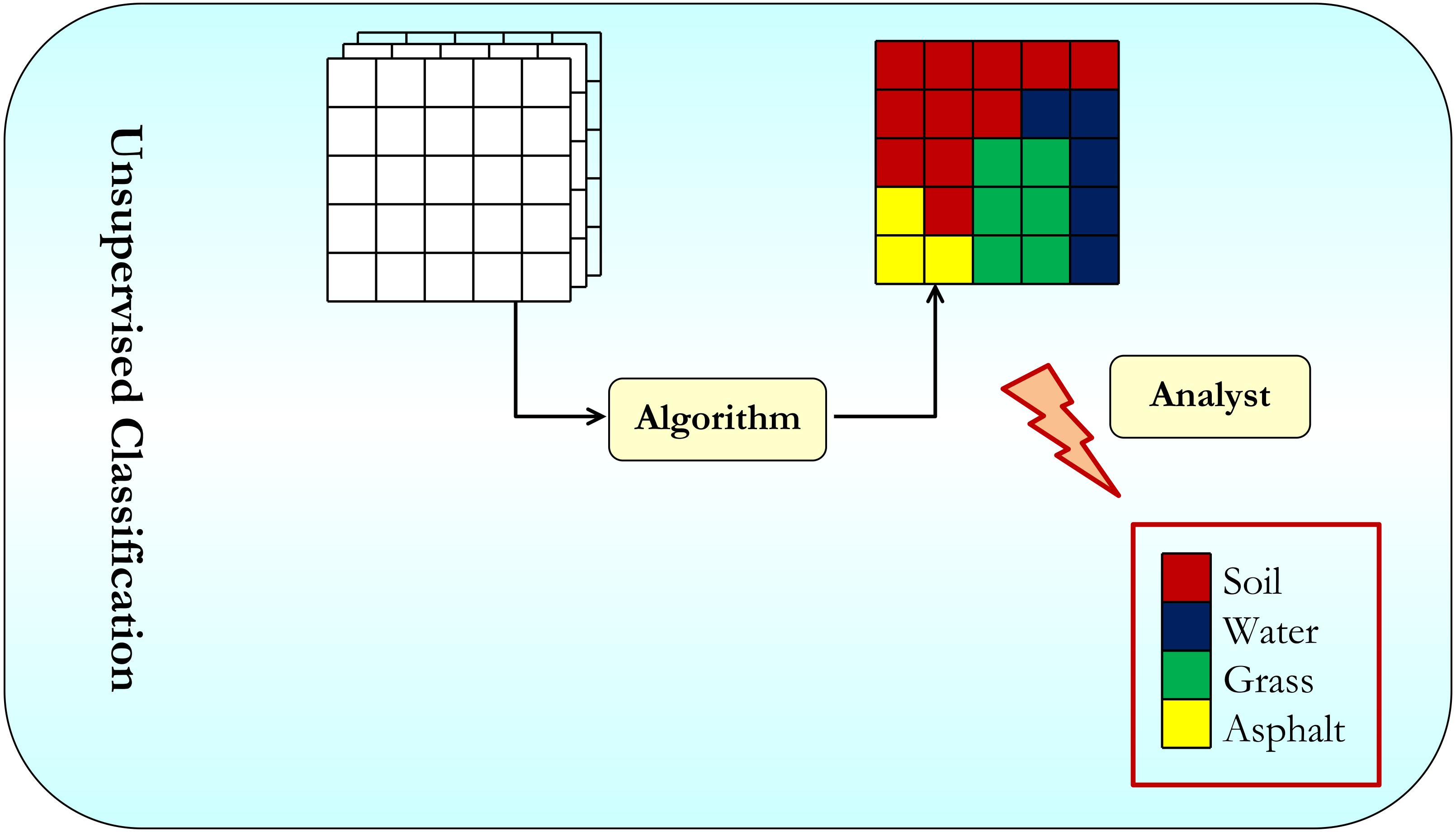

Classification problem

- Given a set of observations (i.e., pixel vectors in a hyperspectral image), the goal of classification is to assign a distinct class label to every pixel in the image.

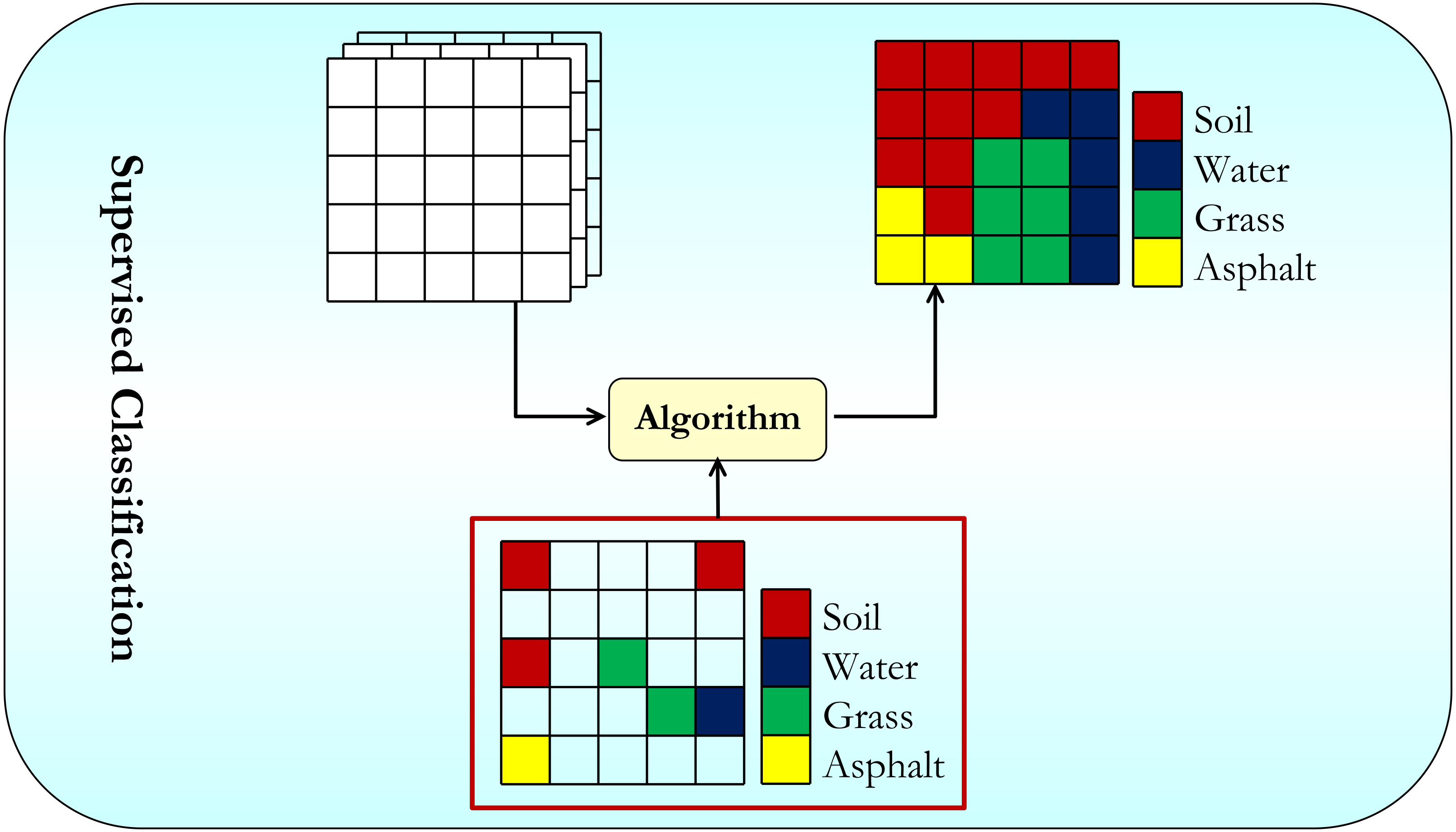

Introduction

- Hyperspectral image classification
- Integration of spatial and spectral information
- Subsapce-based methods
- Data set

The importance of spatial information

- When dealing with hyperspectral images with high spatial resolution, the use of spatial features increases the discrimination of the thematic classes.
- Spectral-spatial classification can lead to significantly more accurate results:

True color image

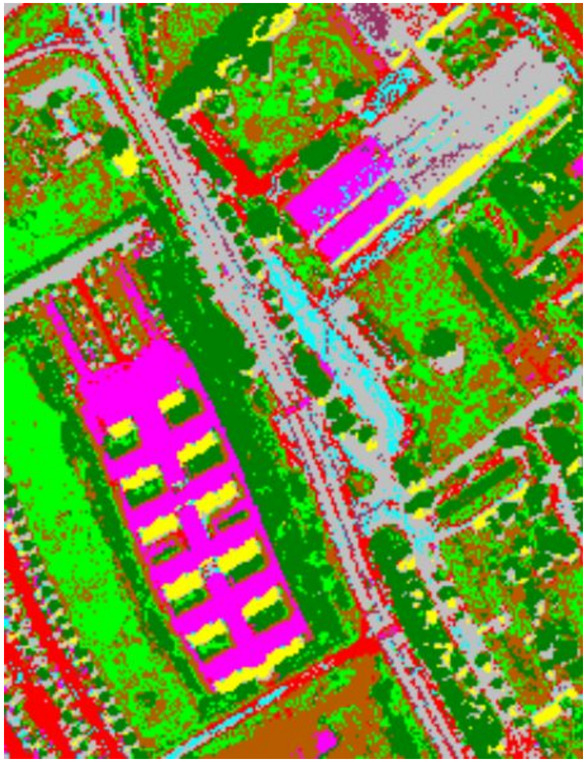

Spectral classification

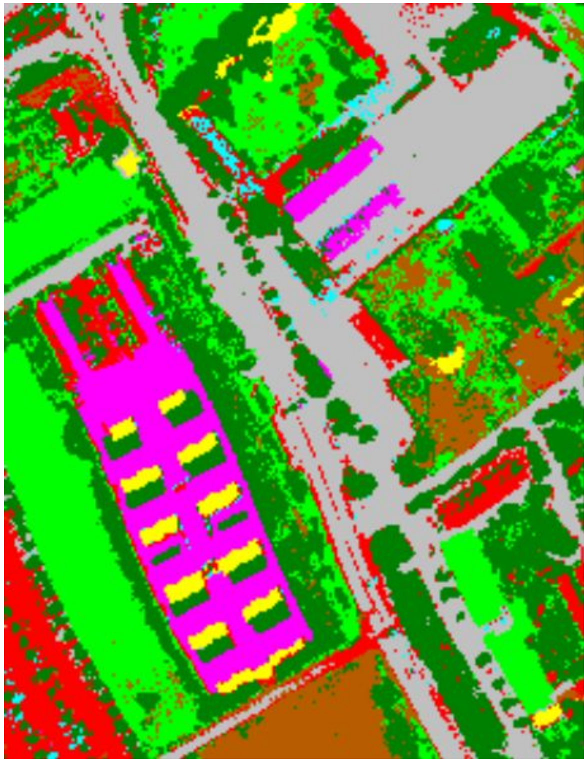

Spectral-spatial classification

The importance of spatial information

- When dealing with hyperspectral images with high spatial resolution, the use of spatial features increases the discrimination of the thematic classes.
- Spectral-spatial classification can lead to significantly more accurate results:

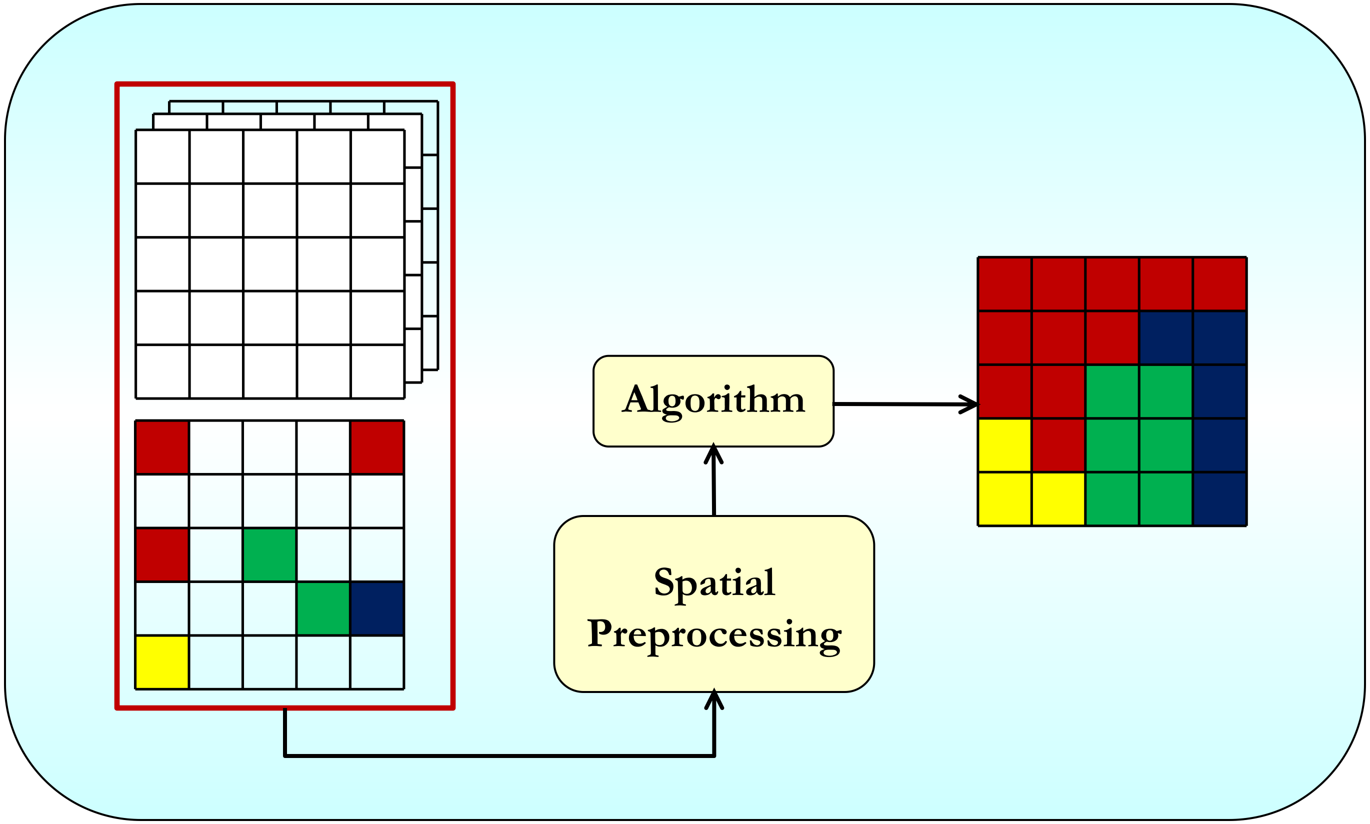

The importance of spatial information

- When dealing with hyperspectral images with high spatial resolution, the use of spatial features increases the discrimination of the thematic classes.
- Spectral-spatial classification can lead to significantly more accurate results:

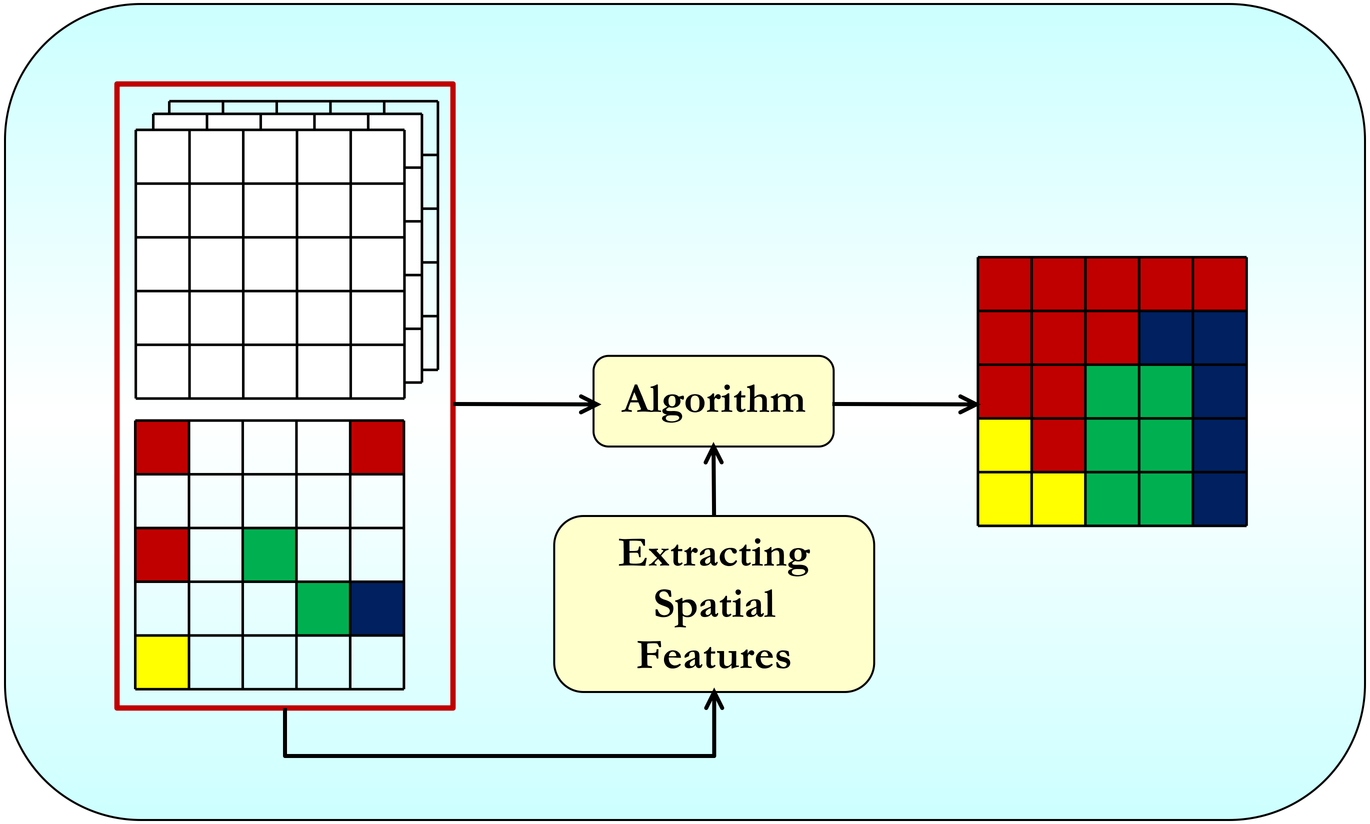

The importance of spatial information

- When dealing with hyperspectral images with high spatial resolution, the use of spatial features increases the discrimination of the thematic classes.
- Spectral-spatial classification can lead to significantly more accurate results:

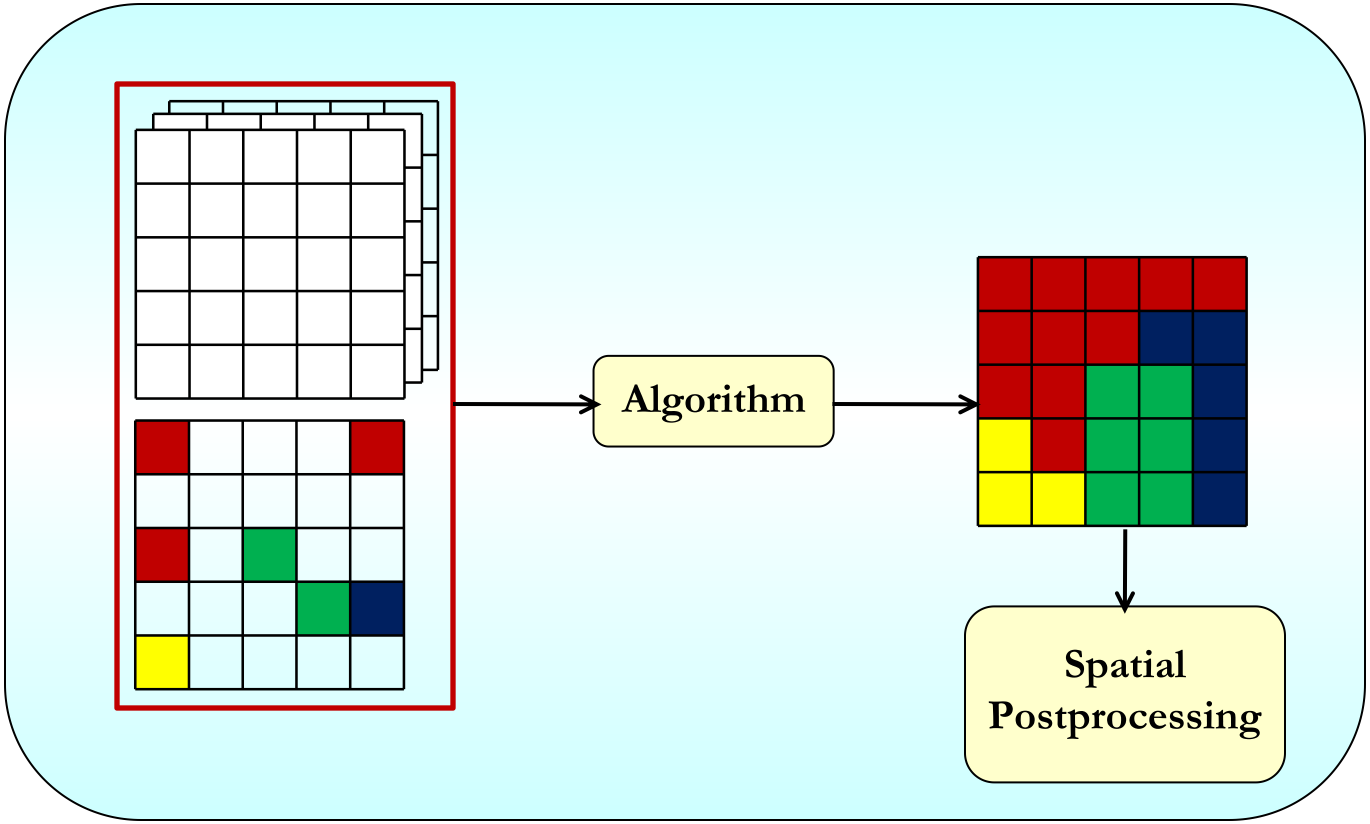

Introduction

- Hyperspectral image classification
- Integration of spatial and spectral information
- Subsapce-based methods
- Data set

Subspace based methods

- It has been proved that the original spectral features in a hyperspectral image contain high redundancy and there is a high correlation between adjacent bands.

Hyperspectral data may effectively live in a lower-dimensional subspace

1. Reducing the dimensionality of hyperspectral data by projecting it to a precise subspace without losing the original spectral information.
2. Increasing the separability of the classes which are very similar in spectral sense.
3. Handling the effects of noise and the presence of heavily mixed pixels in a hyperspectral image.

MLRsub

$$p(y_i = c \mid \mathbf{x}_i, \boldsymbol{\omega}) = \frac{\exp(\boldsymbol{\omega}^{(c)^T} \varphi^{(c)}(\mathbf{x}_i))}{\sum_{c=1}^{K} \exp(\boldsymbol{\omega}^{(c)^T} \varphi^{(c)}(\mathbf{x}_i))}$$

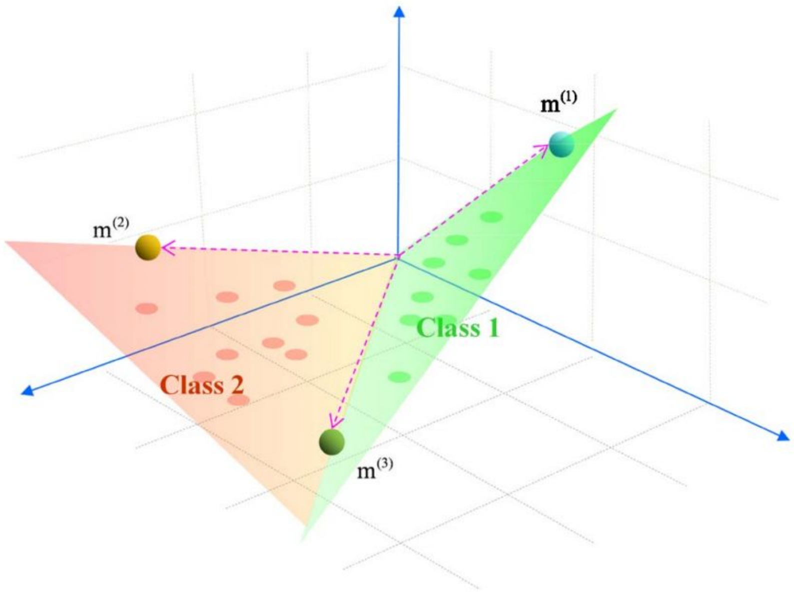

$$\boxed{\varphi^{(c)}(\mathbf{x}_i) = [\|\mathbf{x}_i\|^2, \|\mathbf{x}_i^T \mathbf{U}^{(c)}\|^2]}$$

$\boxed{\mathbf{U}^{(c)}}$: set of lower dimensional orthonormal-basis vectors for the subspace associated with class c using training set $\boxed{D^{(c)}}$

J. Li, J. Bioucas-Dias, and A. Plaza, "Spectral-spatial hyperspectral image segmentation using subspace multinomial logistic regression and Markov random fields," IEEE Transactions on Geoscience and Remote Sensing, vol. 50, no. 3, pp. 809–823, 2012.

Introduction

- Hyperspectral image classification
- Integration of spatial and spectral information
- Subsapce-based methods
- Data set

ROSIS Pavia University data

- Comprises 610x340 pixels and 103 spectral bands between 0.43 and 0.86 microns.
- Spatial resolution of 1.3 meters, with 3921 training samples and 42776 test samples.

False color composition

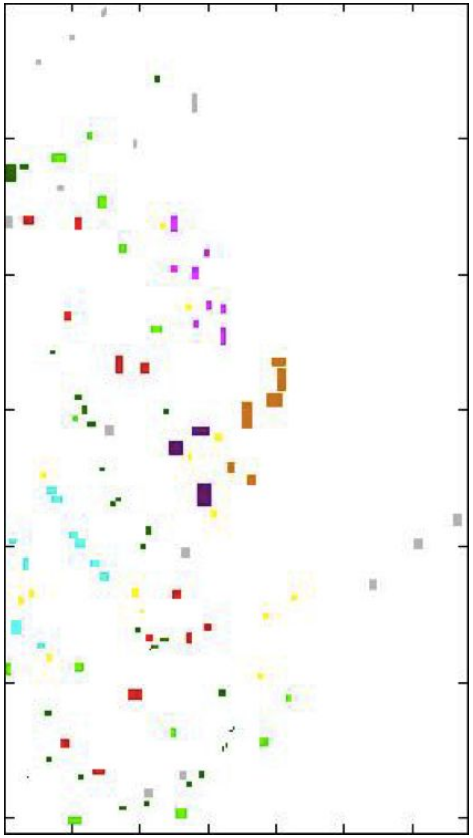

Training data

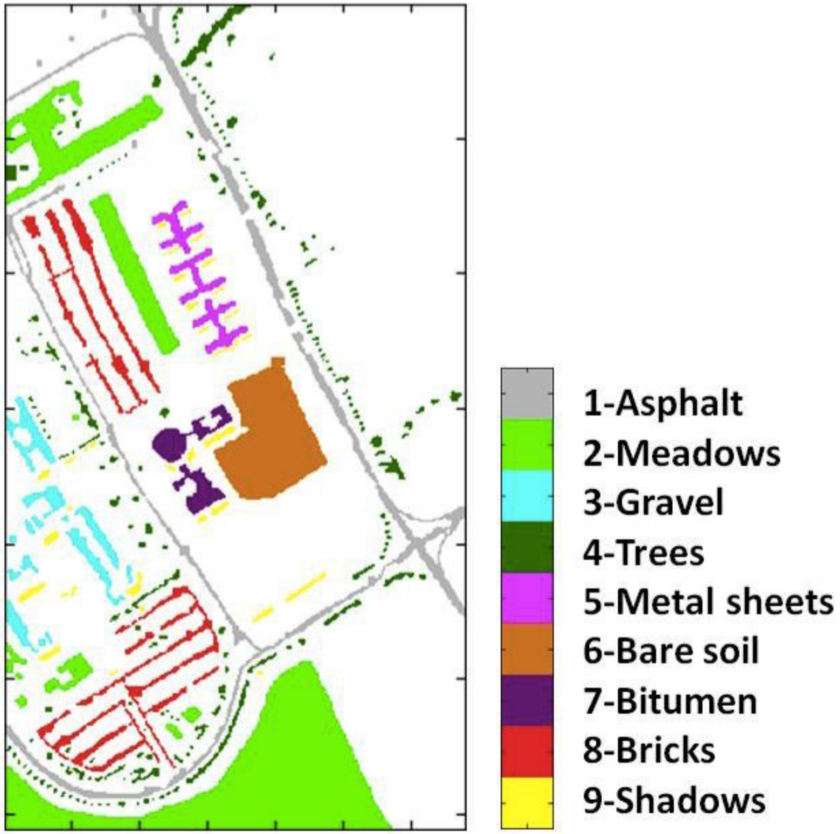

Reference data

Outline

1. Introduction
2. Combining local and global probabilities
3. MLRsub algorithm based on class-indexed subspaces
4. MLRsub algorithm based on union of subspaces
5. Probabilistic relaxation
6. Fusion of hyperspectral and LiDAR data
7. Conclusions and future research lines

Combining local and global probabilities

- ✓ Problem of mixed pixels
- ✓ Multiple classifier system

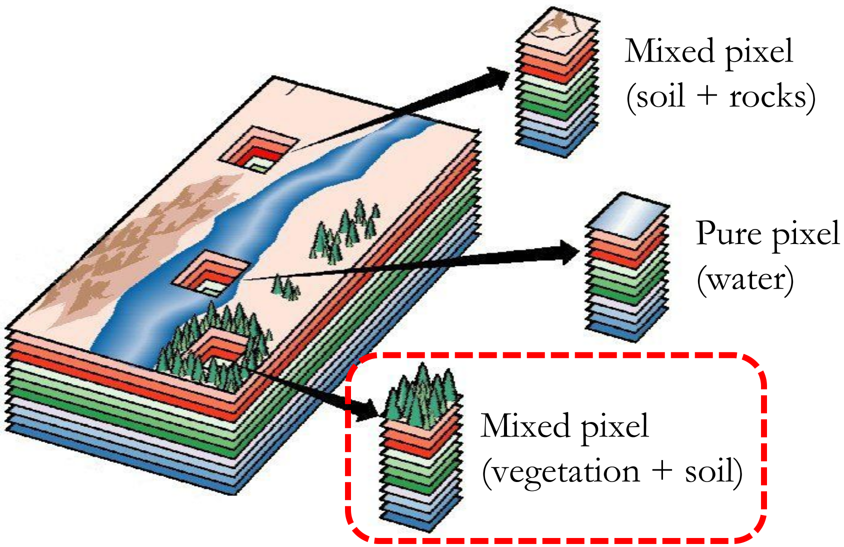

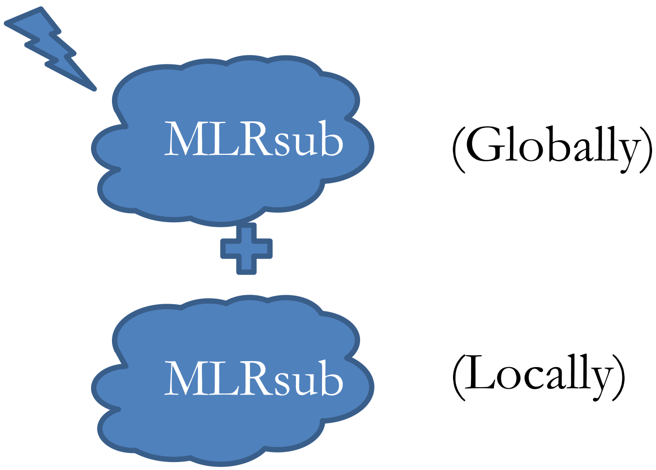

M. Khodadadzadeh, J. Li, A. Plaza, H. Ghassemian, J. M. Bioucas-Dias and X. Li, "Spectral-Spatial Classification of Hyperspectral Data Using Local and Global Probabilities for Mixed Pixel Characterization," IEEE Transactions on Geoscience and Remote Sensing, vol. 52, no. 10, pp. 6298-6314, October 2014.

Combining local and global probabilities

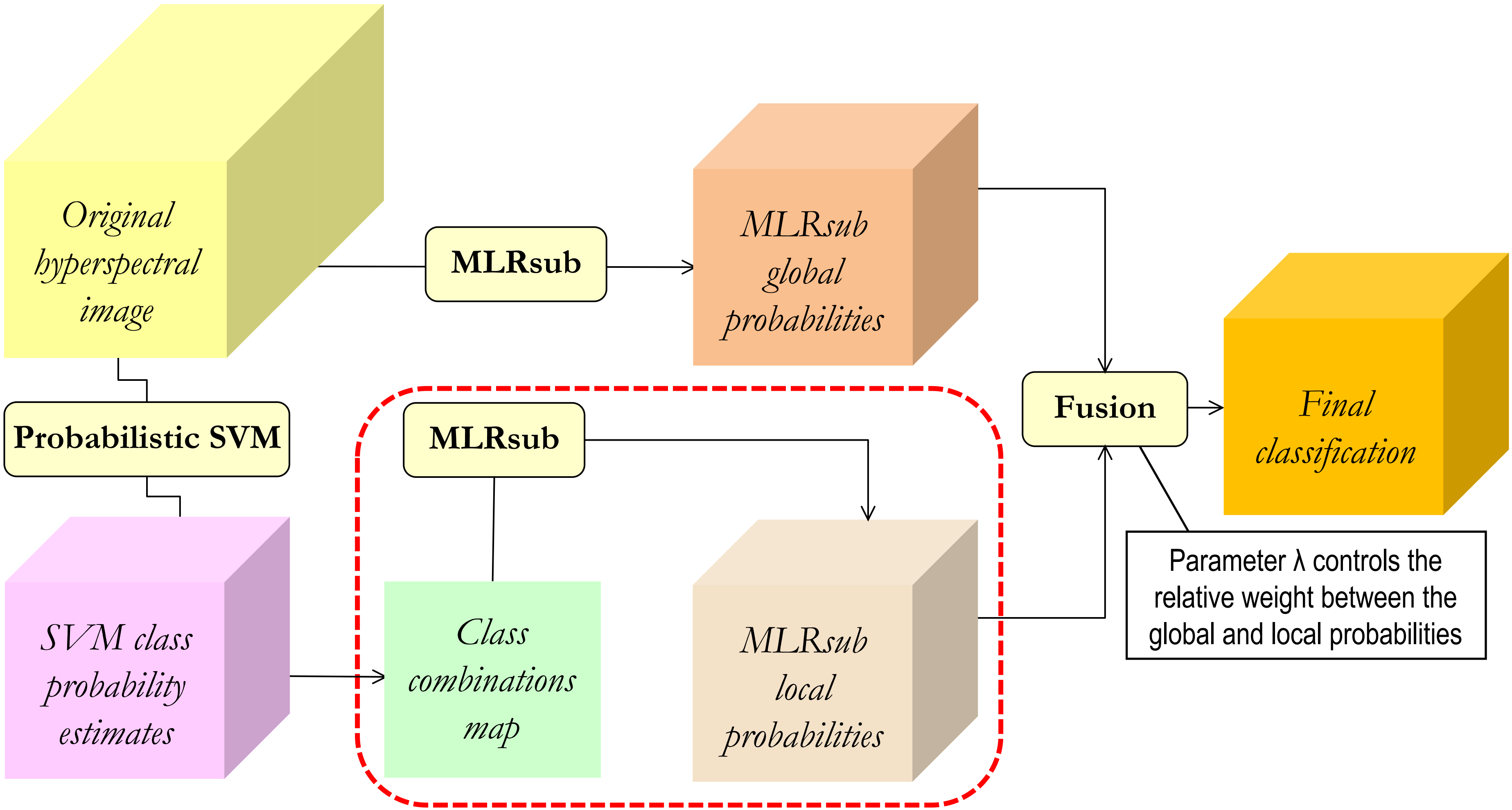

Class combinations map

- Based on the probabilistic SVM results, a subset of the M most reliable class labels is chosen for each pixel as the set of class combination for that pixel, where $M \leq k$ being k the total number of classes.

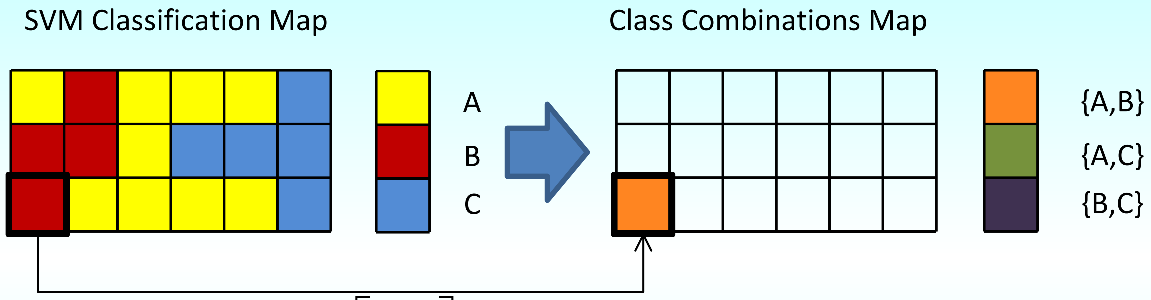

$$P_{SVM} = \begin{bmatrix} 0.3 \\ 0.6 \\ 0.1 \end{bmatrix}$$

Class combinations map

- Based on the probabilistic SVM results, a subset of the M most reliable class labels is chosen for each pixel as the set of class combination for that pixel, where $M \leq k$ being k the total number of classes.

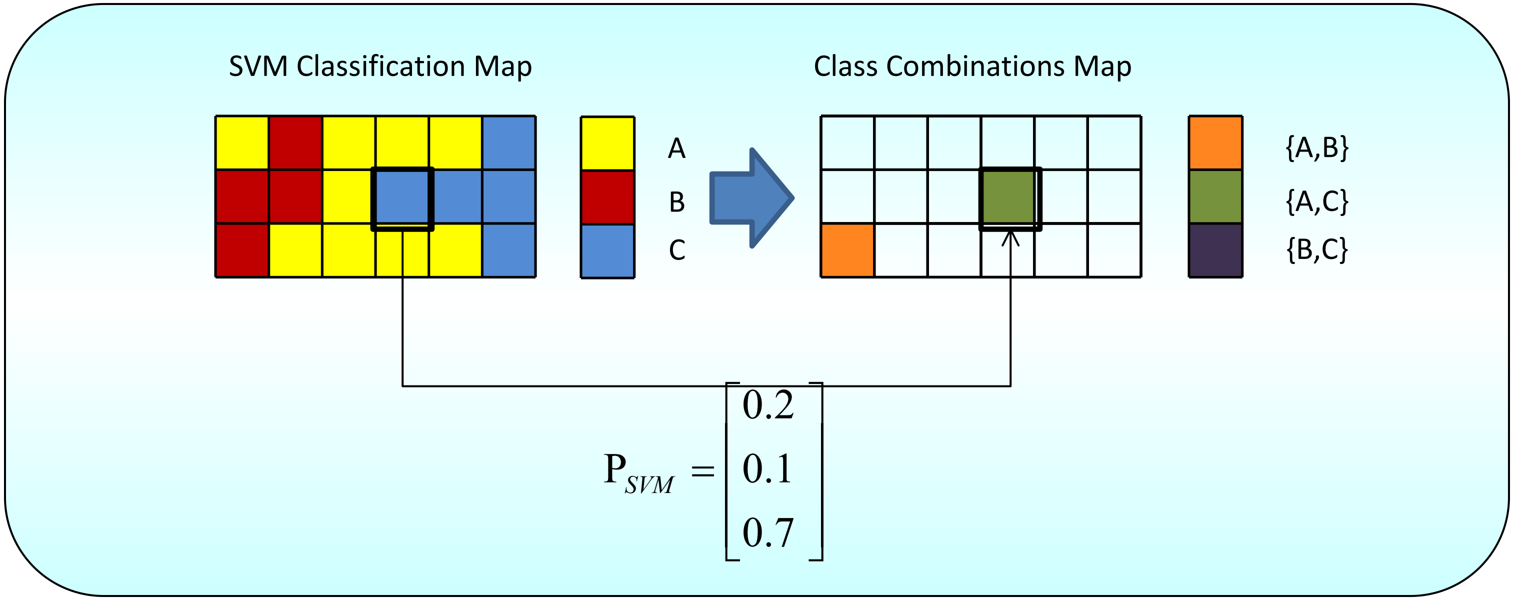

Class combinations map

- Based on the probabilistic SVM results, a subset of the M most reliable class labels is chosen for each pixel as the set of class combination for that pixel, where $M \leq k$ being k the total number of classes.

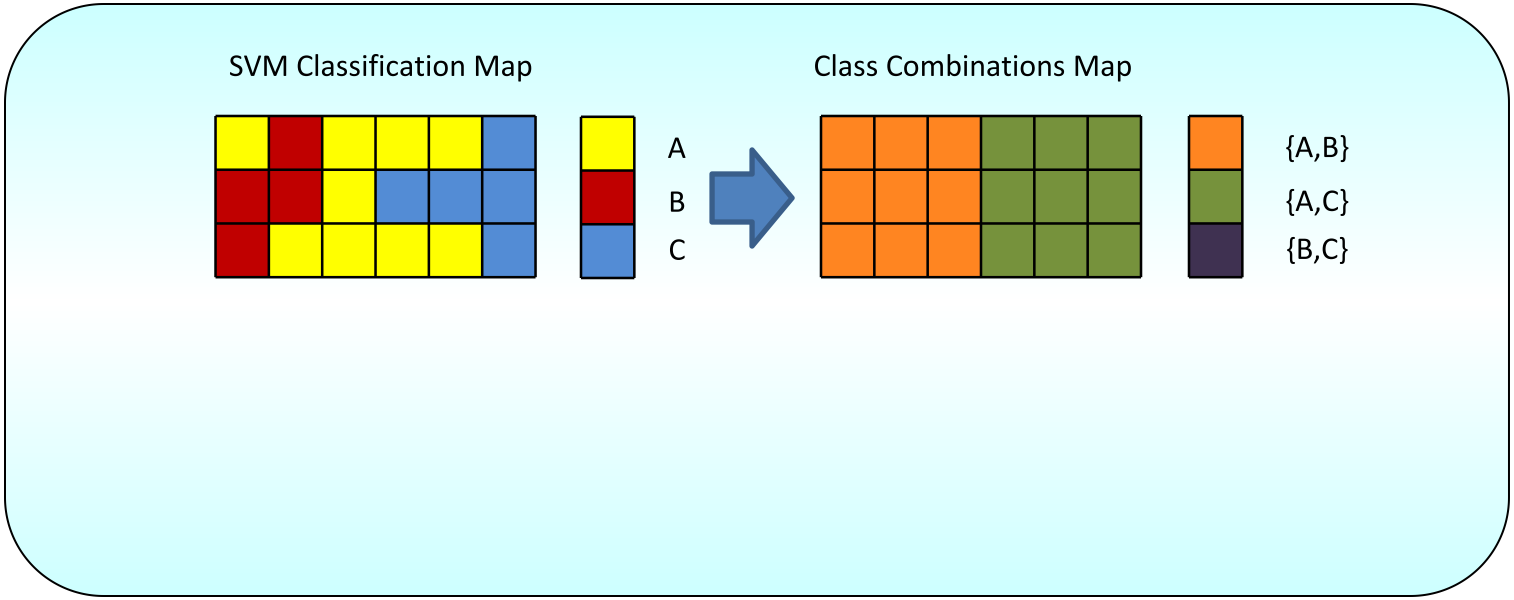

Calculation of the probabilities

- MLRsub algorithm uses to learn the posterior probability distributions locally for the M classes selected in the previous step and globally for all classes.

$$p(y_i = c|\mathbf{x}_i) = \lambda p_g(y_i = c|\mathbf{x}_i, \boldsymbol{\omega}_g) + (1-\lambda)\, p_l(y_i = c|\mathbf{x}_i, \boldsymbol{\omega}_l)$$

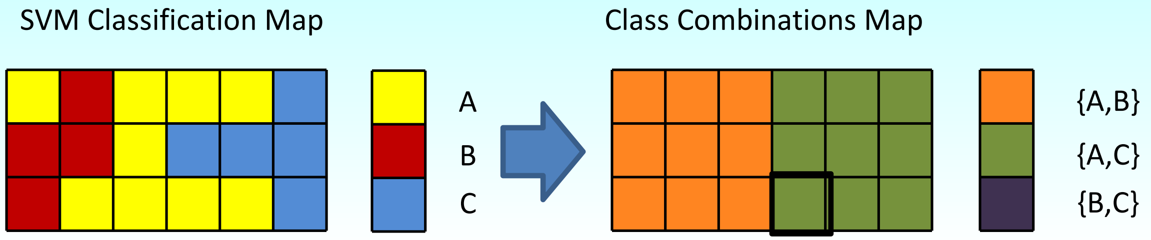

$$P_l = \{p(y_i = A|x_i, \omega_l), 0, p(y_i = C|x_i, \omega_l)\}$$

$$P_g = \{p(y_i = c|x_i, \omega_g), c = A, B, C\}$$

Calculation of the probabilities

- MLRsub algorithm uses to learn the posterior probability distributions locally for the M classes selected in the previous step and globally for all classes.

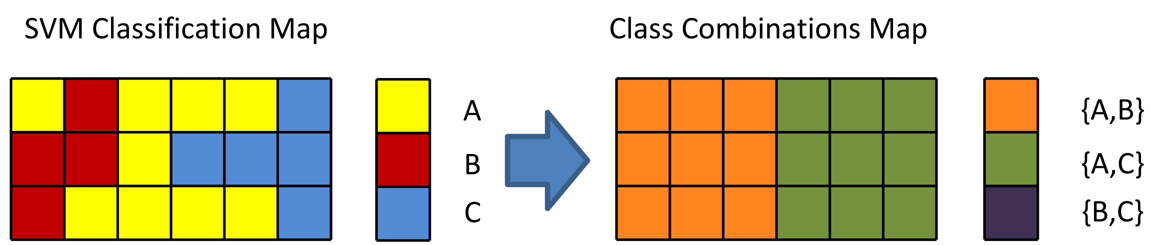

Classification Accuracy	M						
	2	**3**	**4**	**5**	**6**	**7**	**8**
Overall	82.61	78.95	76.07	74.38	72.73	71.94	71.24
Average	83.79	80.31	77.67	76.38	75.25	74.66	74.23

Overall classification accuracies as a function of parameter *M*

Experimental results

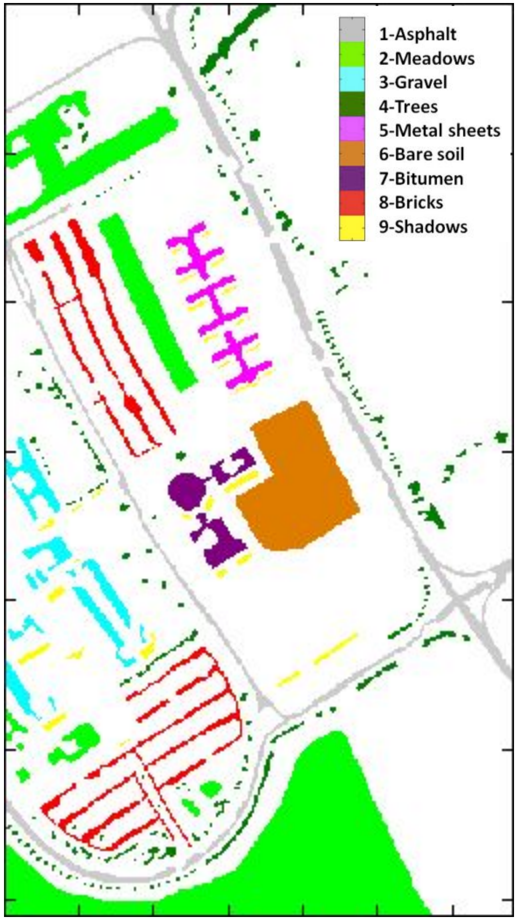

Ground truth map

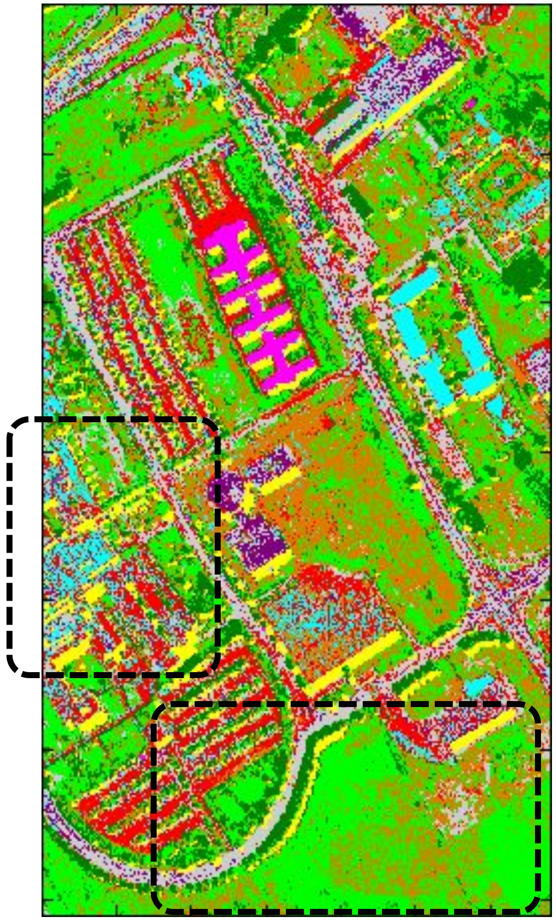

MLRsub(global)
OA=70.61%, AA=73.92%

MLRsub(global+local)
OA=82.61%, AA=83.80%

Outline

Subspace based MLR

- MLRsub method aims to deal with the problems defined by the linear mixing model.

✓ Handling the nonlinearity of the mixtures

By assuming dependence between the class-indexed subspaces

$$p(y_i = c | \mathbf{x}_i, \boldsymbol{\omega}) = \frac{\exp(\boldsymbol{\omega}^{(c)^T} \varphi^{(c)}(\mathbf{x}_i))}{\sum_{c=1}^{K} \exp(\boldsymbol{\omega}^{(c)^T} \varphi^{(c)}(\mathbf{x}_i))}$$

$$\varphi^{(c)}(\mathbf{x}_i) = [\| \mathbf{x}_i \|^2, \| \mathbf{x}_i^{\mathrm{T}} \mathbf{U}^{(c)} \|^2]$$

M. Khodadadzadeh, J. Li, A. Plaza and J. M. Bioucas-Dias, "A Subspace Based Multinomial Logistic Regression for Hyperspectral Image Classification," IEEE Geoscience and Remote Sensing Letters, vol. 11 no. 12, pp. 2105-2109, December 2014.

Subspace based MLR

- MLRsub method aims to deal with the problems defined by the linear mixing model.

✓ Handling the nonlinearity of the mixtures

By assuming dependence between the class-indexed subspaces

$$p(y_i = c|\mathbf{x}_i, \boldsymbol{\omega}) = \frac{\exp(\boldsymbol{\omega}^{(c)^T} \varphi(\mathbf{x}_i))}{\sum_{c=1}^{K} \exp(\boldsymbol{\omega}^{(c)^T} \varphi(\mathbf{x}_i))}$$

$$\varphi(\mathbf{x}_i) = [\|\mathbf{x}_i\|^2, \|\mathbf{x}_i^{\mathrm{T}} \mathbf{U}^{(1)}\|^2, \ldots, \|\mathbf{x}_i^{\mathrm{T}} \mathbf{U}^{(K)}\|^2]$$

Subspace based MLR

- MLRsub method aims to deal with the problems defined by the linear mixing model

✓ Handling the nonlinearity of the mixtures

✓ Using the available prior knowledge about classes

By including the class prior probabilities

$$p(y_i = c | \mathbf{x}_i, \boldsymbol{\omega}) = \frac{\exp(\boldsymbol{\omega}^{(c)^T} \varphi(\mathbf{x}_i))}{\sum_{c=1}^{K} \exp(\boldsymbol{\omega}^{(c)^T} \varphi(\mathbf{x}_i))}$$

$$\boxed{\varphi(\mathbf{x}_i) = [\| \mathbf{x}_i \|^2, \| \mathbf{x}_i^{\mathrm{T}} \mathbf{U}^{(1)} \|^2, \ldots, \| \mathbf{x}_i^{\mathrm{T}} \mathbf{U}^{(K)} \|^2]}$$

Subspace based MLR

- MLRsub method aims to deal with the problems defined by the linear mixing model

✓ Handling the nonlinearity of the mixtures

✓ Using the available prior knowledge about classes

By including the class prior probabilities

$$p(y_i = c | \mathbf{x}_i, \boldsymbol{\omega}) = \frac{\exp(\boldsymbol{\omega}^{(c)^T} \varphi(\mathbf{x}_i)) p(y_i = c)}{\sum_{c=1}^{K} \exp(\boldsymbol{\omega}^{(c)^T} \varphi(\mathbf{x}_i)) p(y_i = l)}$$

$$\varphi(\mathbf{x}_i) = [\| \mathbf{x}_i \|^2, \| \mathbf{x}_i^{\mathrm{T}} \mathbf{U}^{(1)} \|^2, \ldots, \| \mathbf{x}_i^{\mathrm{T}} \mathbf{U}^{(K)} \|^2]$$

$$p(y_i = c) = \frac{n_{tr}^{(c)}}{n_{tr}}$$

Experimental results

Ground truth map

MLRsub
OA=70.61%, AA=73.92%

MLRsubmod
OA=78.49%, AA=82.41%

Outline

1. Introduction
2. Combining local and global probabilities
3. MLRsub algorithm based on class-indexed subspaces
4. MLRsub algorithm based on union of subspaces
5. Probabilistic relaxation
6. Fusion of hyperspectral and LiDAR data
7. Conclusions and future research lines

Union of Subspaces

- Modeling high-dimensional data with a union of subspaces is a useful generalization of subspace models.

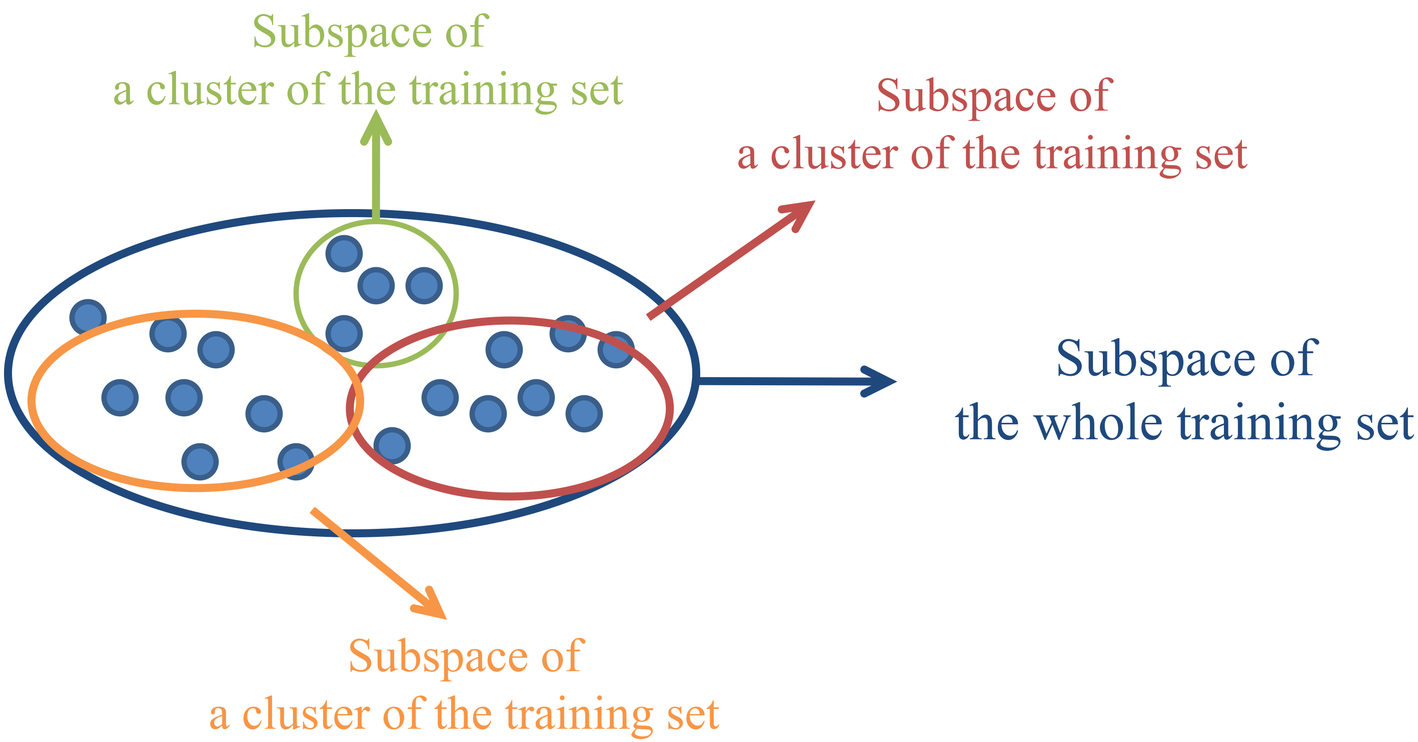

M. Khodadadzadeh, J. Li, A. Plaza and J. M. Bioucas-Dias, "Hyperspectral Image Classification Based on Union of Subspaces," IEEE Joint Urban Remote Sensing Event (JURSE'15), Lausanne, Switzerland, 2015.

- Includes: 1) subspace clustering of training samples set; 2) subspace projection and probabilistic classification using MLR algorithm.

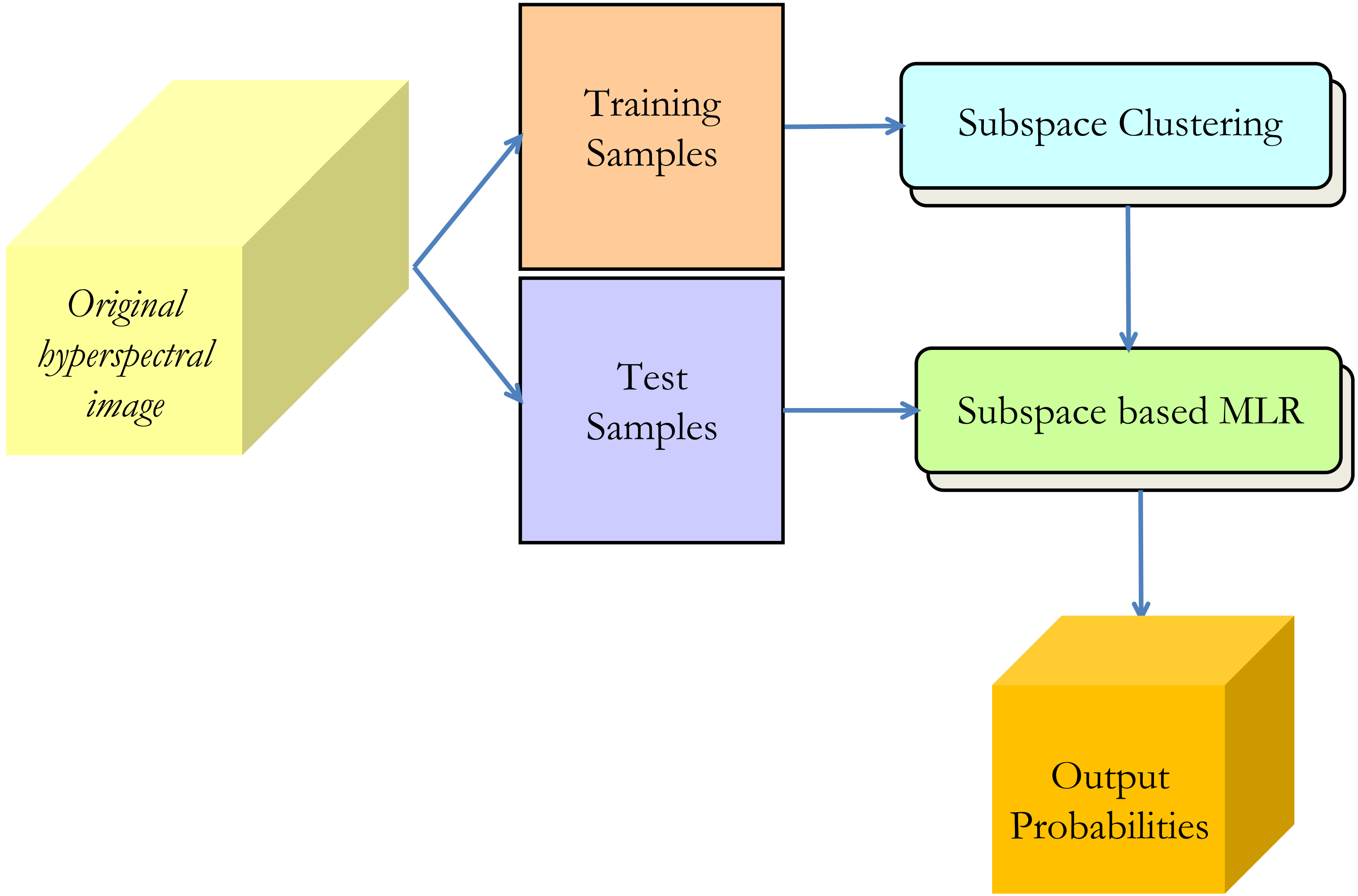

M. Soltanolkotabi, E. Elhamifar, E. J. Candes et al., “Robust subspace clustering,” The Annals of Statistics, vol. 42, no. 2, pp. 669–699, 2014.

Union of Subspaces MLR

- Exploiting the union of subspaces in an MLR framework by including the norms of the projection of the spectral vectors onto the subspaces estimated by RSC.

$$p(y_i = c|\mathbf{x}_i, \boldsymbol{\omega}) = \frac{\exp(\boldsymbol{\omega}^{(c)^T} \varphi(\mathbf{x}_i))}{\sum_{c=1}^{K} \exp(\boldsymbol{\omega}^{(c)^T} \varphi(\mathbf{x}_i))}$$

$$\varphi(\mathbf{x}_i) = [\| \mathbf{x}_i \|^2, \| \mathbf{x}_i^{\mathrm{T}} \mathbf{U}^{(1)} \|^2, \ldots, \| \mathbf{x}_i^{\mathrm{T}} \mathbf{U}^{(K)} \|^2]$$

$$\Downarrow$$

$$\varphi(\mathbf{x}_i) = [\| \mathbf{x}_i \|^2, \| \mathbf{x}_i^{\mathrm{T}} \mathbf{U}_1^{(1)} \|^2, \ldots, \| \mathbf{x}_i^{\mathrm{T}} \mathbf{U}_{L^{(1)}}^{(1)} \|^2, \ldots, \| \mathbf{x}_i^{\mathrm{T}} \mathbf{U}_1^{(K)} \|^2, \ldots, \| \mathbf{x}_i^{\mathrm{T}} \mathbf{U}_{L^{(K)}}^{(K)} \|^2]$$

Experimental results

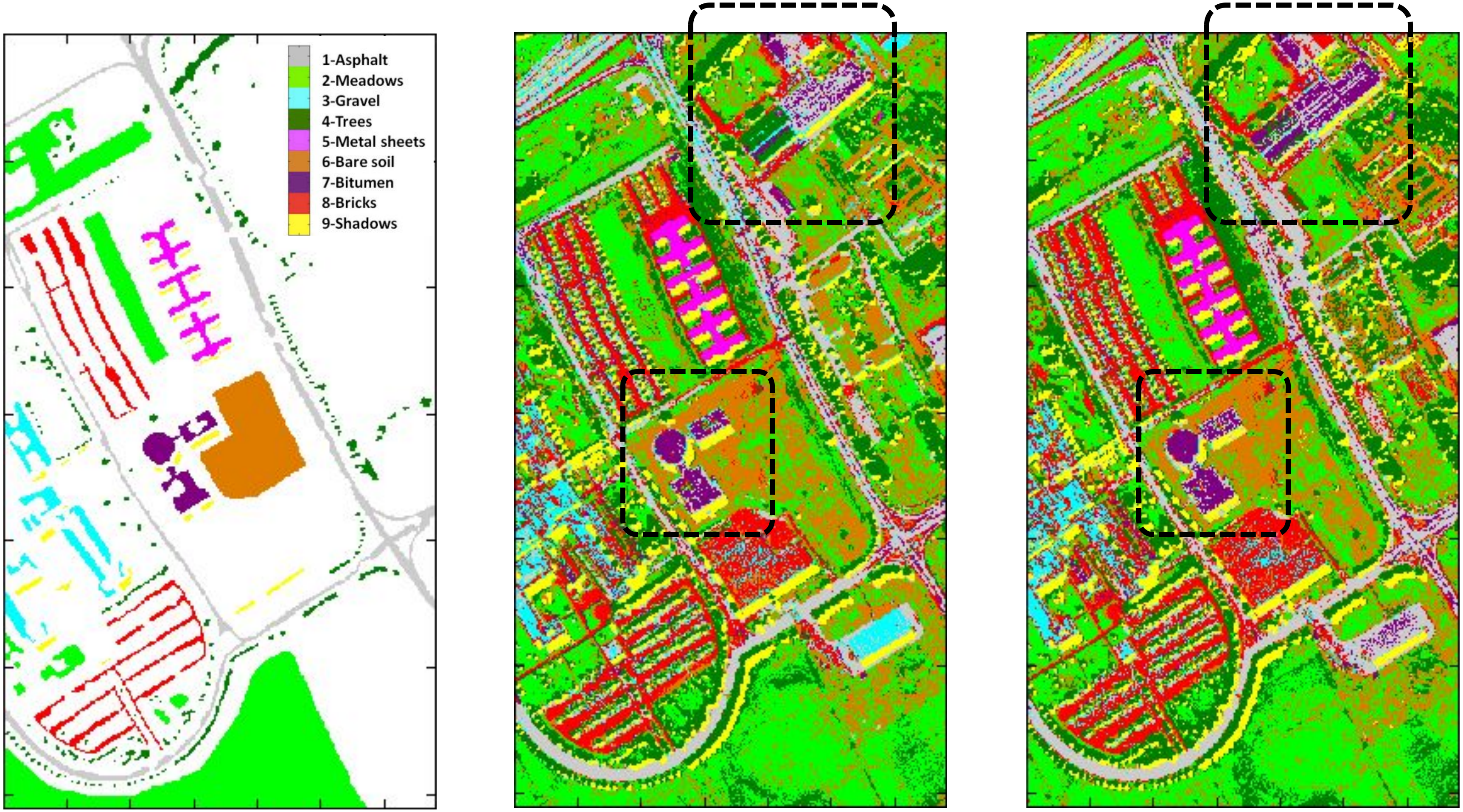

Ground truth map

MLRsubmod
OA=78.49%, AA=82.41%

MLRUsub
OA=80.24%, AA=83.95%

Outline

1. Introduction
2. Combining local and global probabilities
3. MLRsub algorithm based on class-indexed subspaces
4. MLRsub algorithm based on union of subspaces
5. Probabilistic relaxation
6. Fusion of hyperspectral and LiDAR data
7. Conclusions and future research lines

Relaxation

- As preprocessing, spatial smoothing over the hyperspectral data can remove noise and enhance spatial texture information.
- As postprocessing, relaxation-based approaches can be an effective tool to improve classification accuracies.

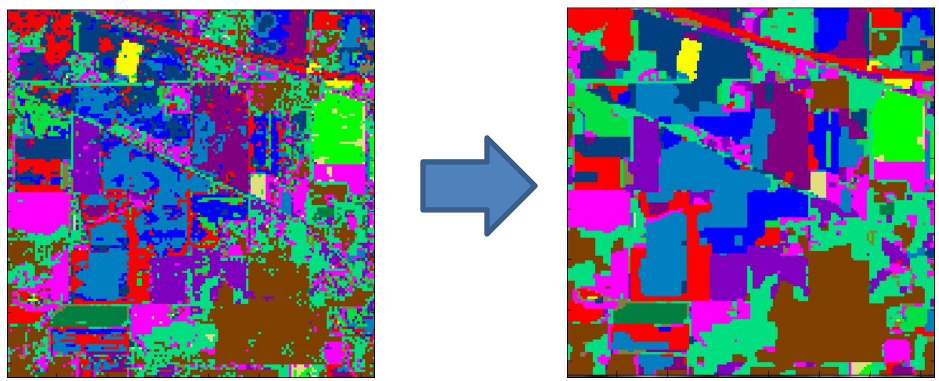

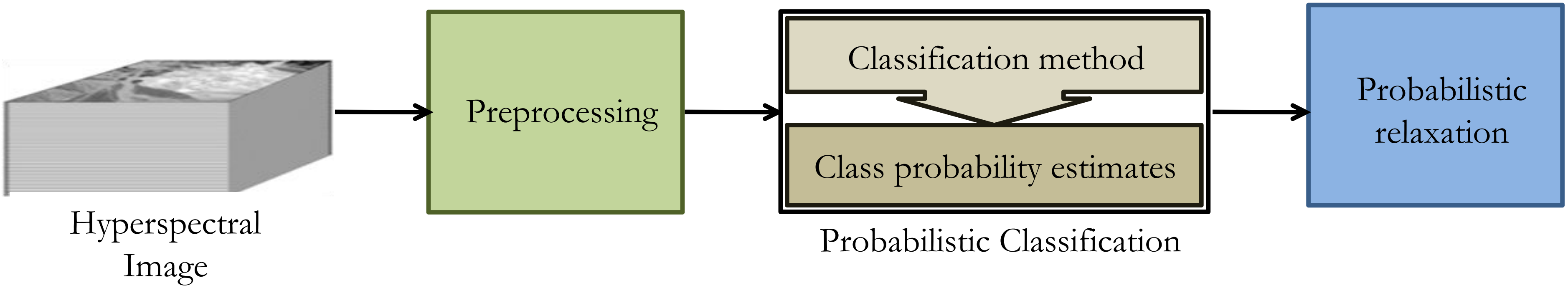

J. Li, M. Khodadadzadeh, A. Plaza, X. Jia and J. M. Bioucas-Dias, "A Discontinuity Preserving Relaxation scheme for Spectral-Spatial Hyperspectral Image Classification," IEEE Journal of Selected Topics in Applied Earth Observations and Remote Sensing, 2015.

Relaxation

- ➕ Improves the classification accuracy in smooth image areas.
- ➖ Degrades the classification performance in the neighborhood of the class boundaries.

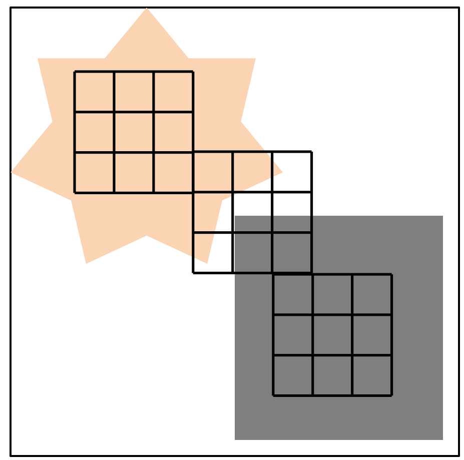

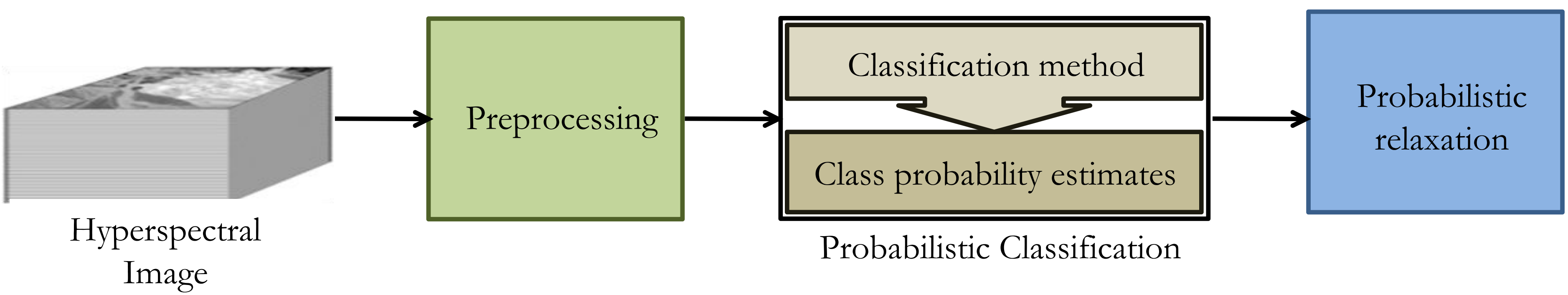

Discontinuity Preserving Relaxation

- Improves the classification accuracy in smooth image areas.
- Degrades the classification performance in the neighborhood of the class boundaries.

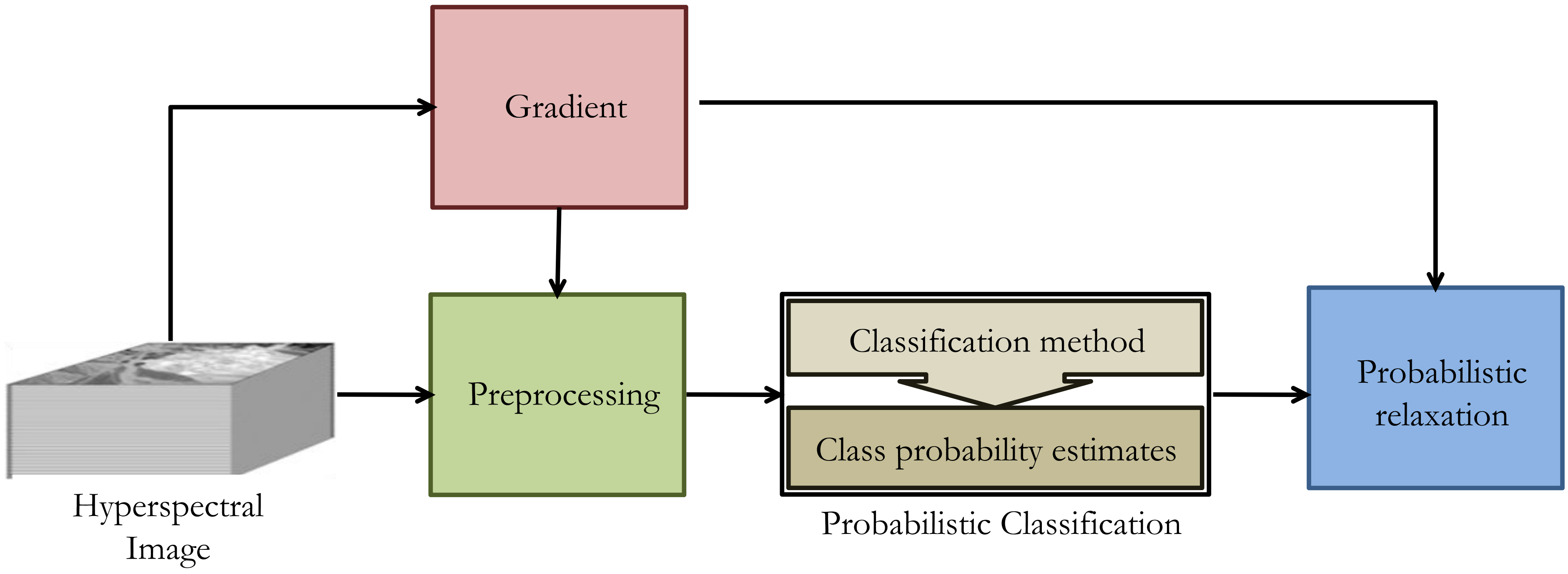

Discontinuity Preserving Relaxation

- We implement a relaxation scheme that is the solution of the following optimization problem:

$$\mathbf{p} = [\mathbf{p}_1, \ldots, \mathbf{p}_n] \in \Re^{K \times n}$$

$$\min \quad (1-\lambda)\|\mathbf{u}-\mathbf{p}\|^2 + \lambda \sum_i \sum_{j \in \partial_i} \varepsilon_j \|\mathbf{u}_j - \mathbf{u}_i\|^2$$

$$s.t.: \quad \mathbf{u}_i \geq 0,\ \mathbf{1}^T \mathbf{u}_i = 1$$

$$\varepsilon = \exp\left(-\sum_{i=1}^{d} sobel(\mathbf{X}^{(i)}) \right)$$

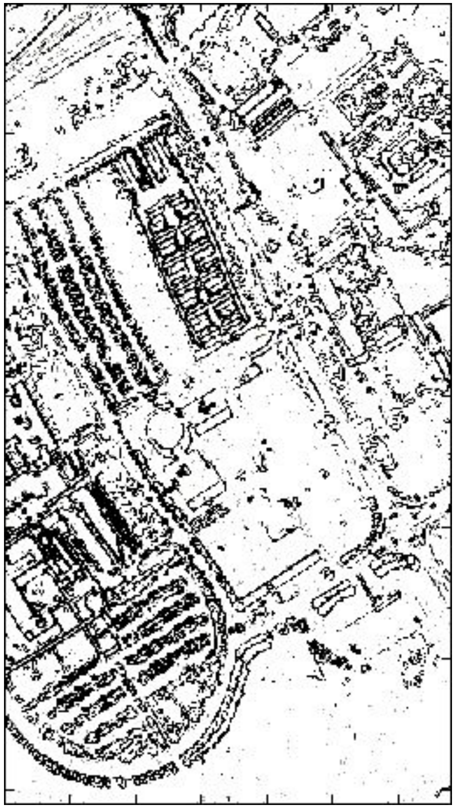

Discontinuity Map

- Using iterative Gauss Seidel method:

$$u_i^{(t+1)}(c) = \frac{(1-\lambda) p_i(c) + \lambda \sum_{j \in \partial_i} \varepsilon_j u_j^{(t)}(c)}{(1-\lambda) + \lambda \sum_{j \in \partial_i} \varepsilon_j}$$

Experimental results

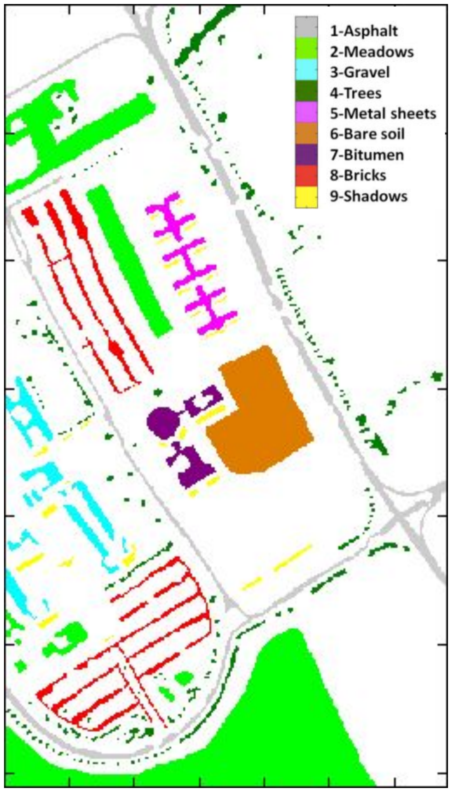

Ground truth map

SVM
OA=81.13%,
AA=89.05%

MLRsub
OA=70.61%,
AA=73.92%

MLRsub(gl)
OA=82.61%,
AA=83.80%

Experimental results

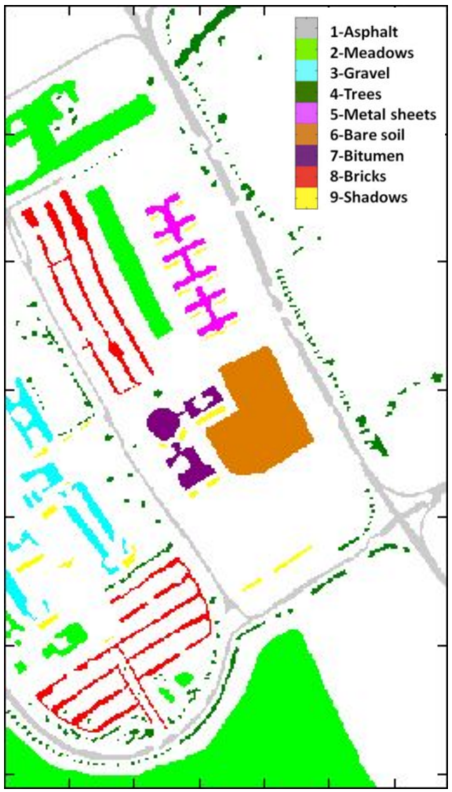

Ground truth map

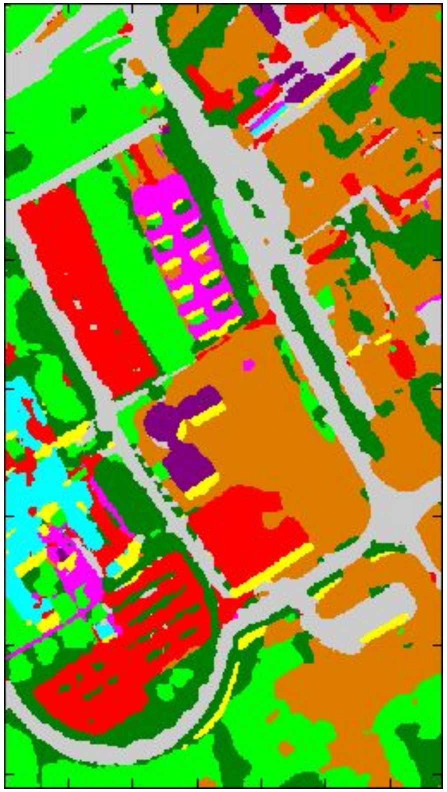

SVM-pr
OA=88.09%,
AA=93.24%

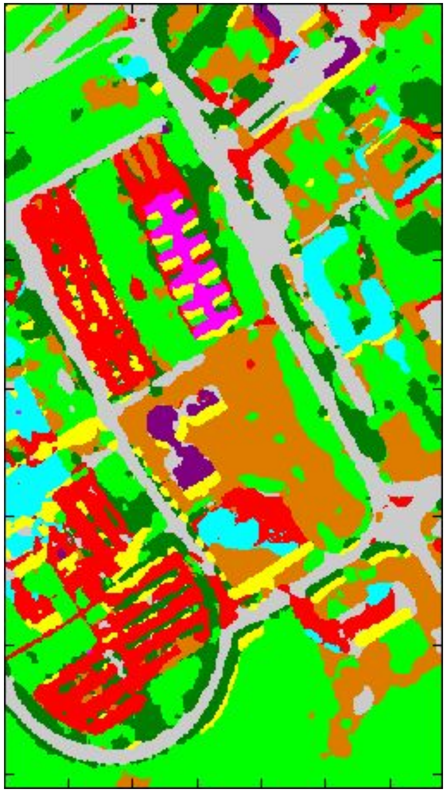

MLRsub-pr
OA=91.93%,
AA=88.39%

MLRsub(gl)-pr
OA=95.05%
AA=92.48%

Experimental results

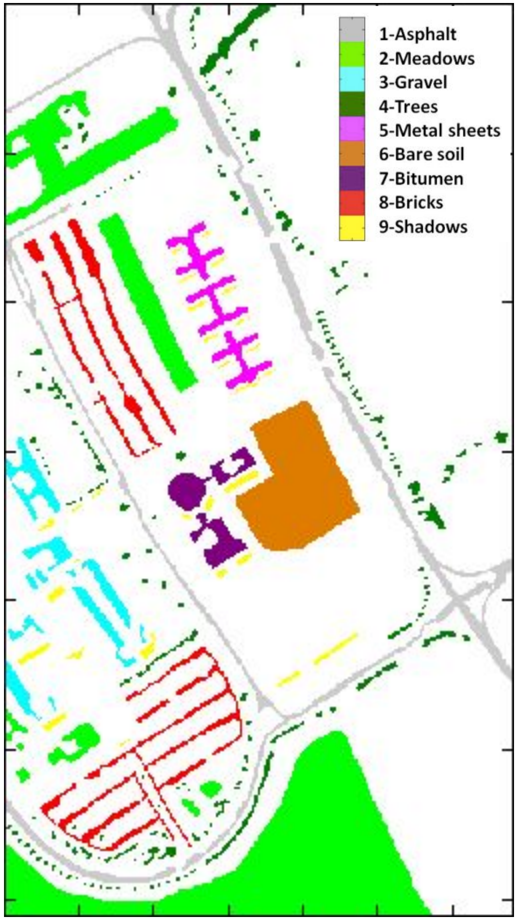

Ground truth map

MLRsubmod
OA=78.49%, AA=82.41%

MLRUsub
OA=80.24%, AA=83.95%

Experimental results

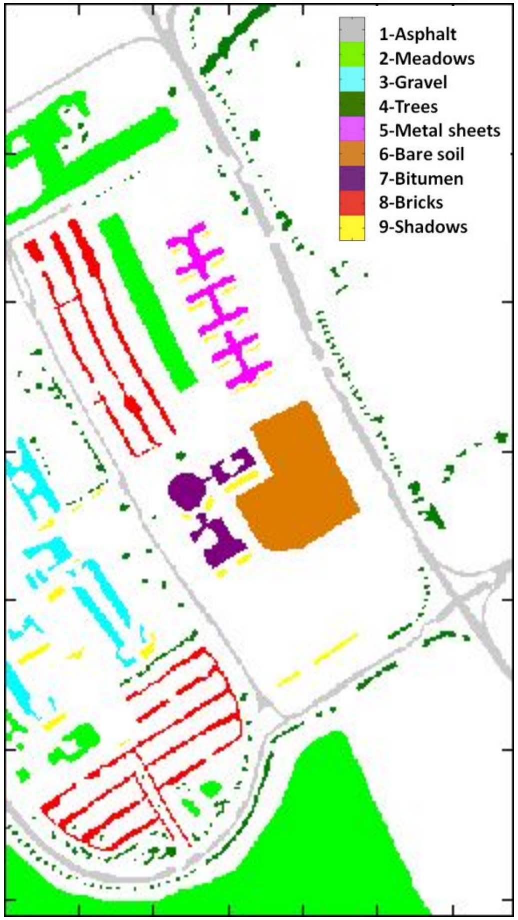

Ground truth map

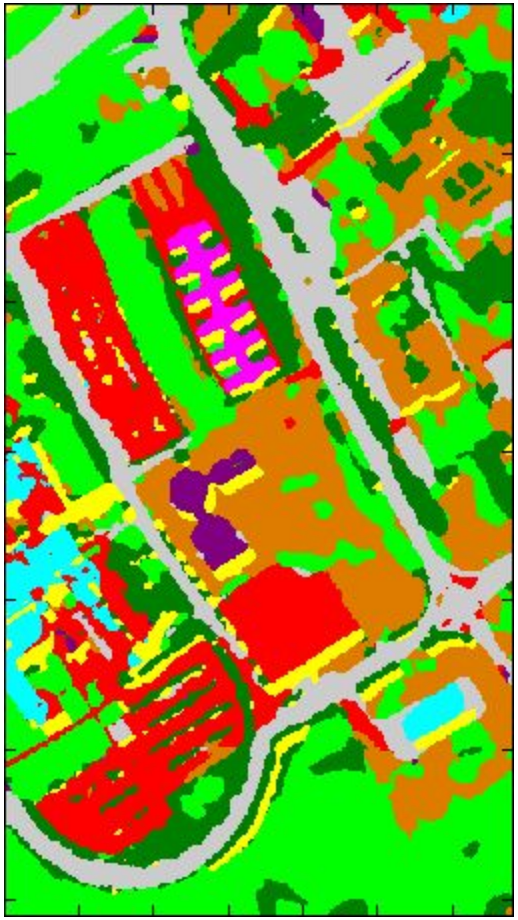

MLRsubmod-pr
OA=92.67%, AA=91.99%

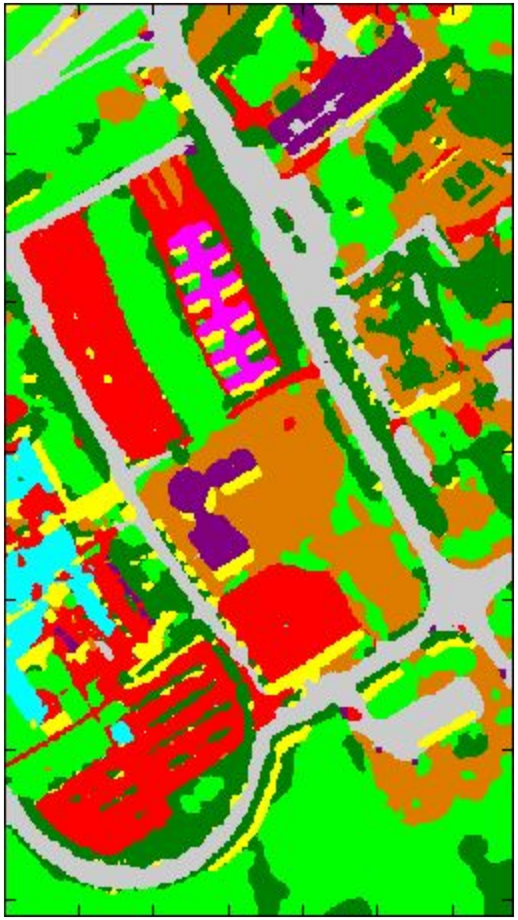

MLRUsub-pr
OA=93.47%, AA=93.14%

Outline

1. Introduction
2. Combining local and global probabilities
3. MLRsub algorithm based on class-indexed subspaces
4. MLRsub algorithm based on union of subspaces
5. Probabilistic relaxation
6. Fusion of hyperspectral and LiDAR data
7. Conclusions and future research lines

Hyperspectral and LiDAR

- Light detection and ranging (LiDAR) provide detailed information on the elevation of the Earth's surface and objects on the landscape.
- Combining information from multiple sources is an effective way to improve classification results.

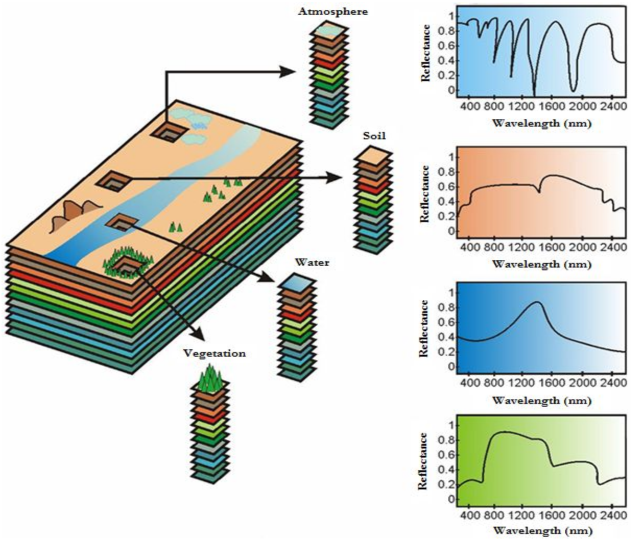

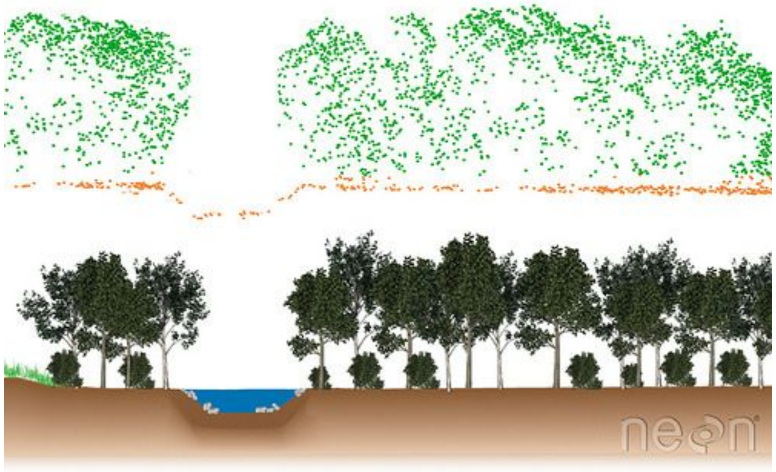

M. Khodadadzadeh, J. Li, S. Prasad and A. Plaza, "Fusion of Hyperspectral and LiDAR Remote Sensing Data Using Multiple Feature Learning," IEEE Journal of Selected Topics in Applied Earth Observations and Remote Sensing, 2015.

The importance of the fusion

- The information provided by LiDAR can effectively complement the spectral information from the hyperspectral data for classification purposes:

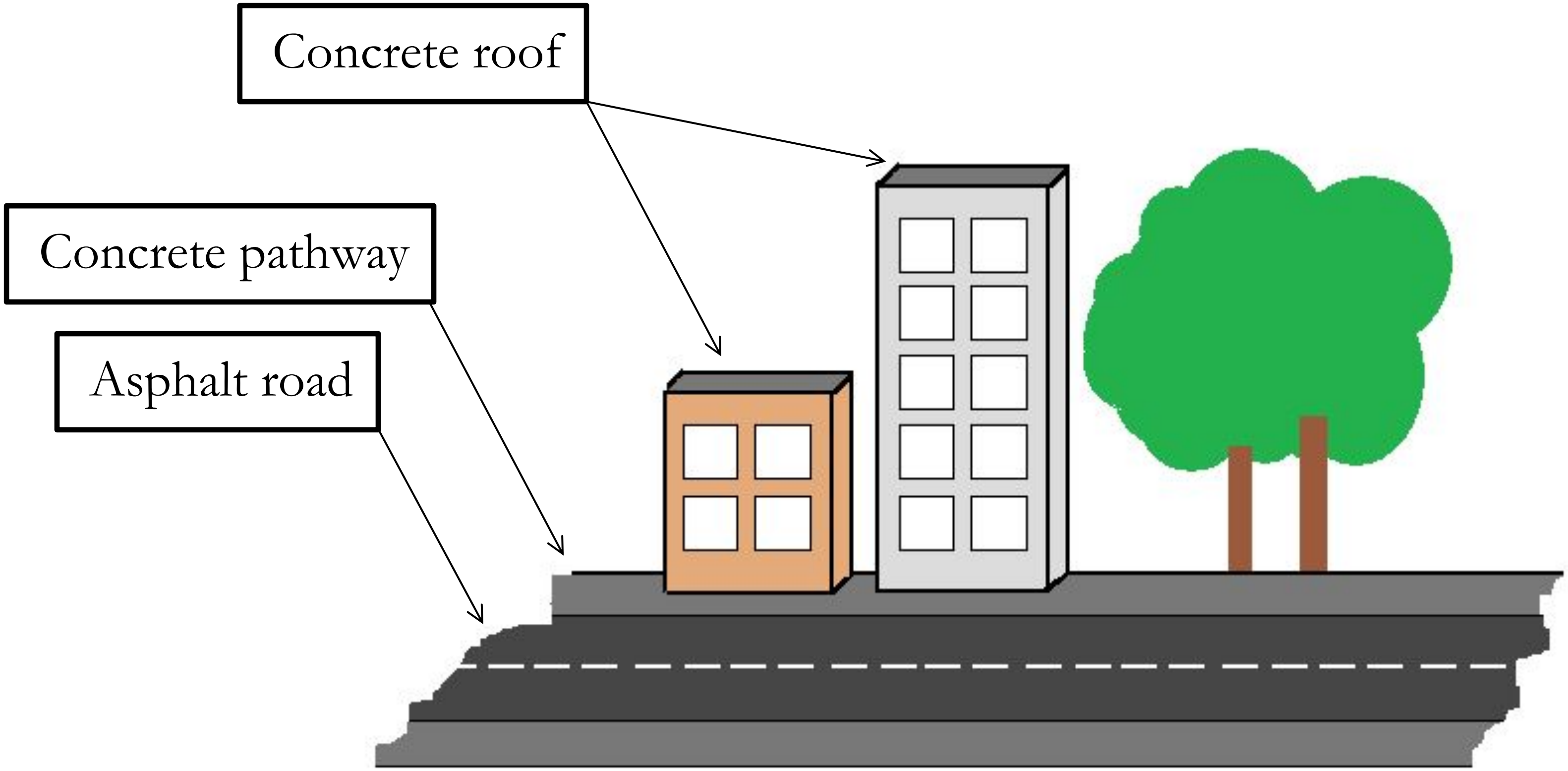

Fusion of hyperspectral and LiDAR data

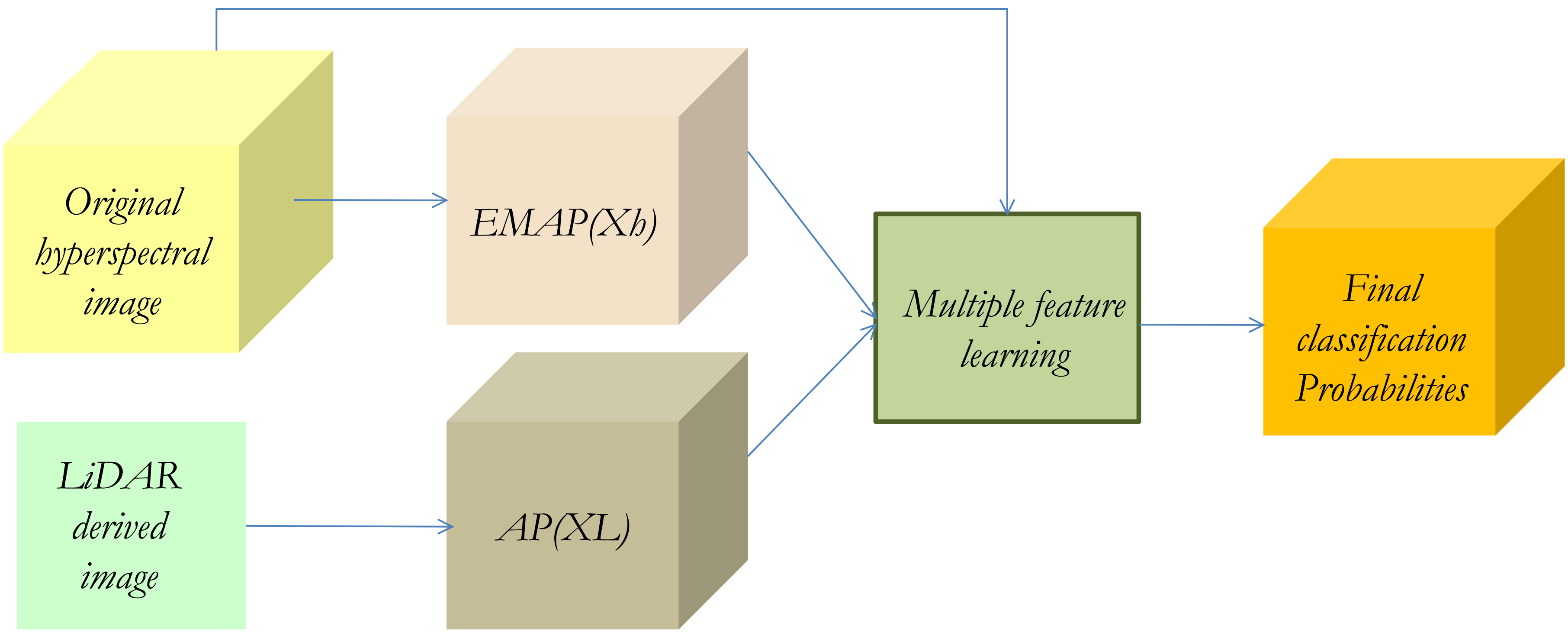

M. Dalla Mura, J. A. Benediktsson, B, Waske and L. Bruzzone, "Morphological attribute profiles for the analysis of very high resolution images," *IEEE Transactions on Geoscience and Remote Sensing*, vol. 48, no. 10, pp. 3747-3762, 2010.

Logarithmic opinion pool (LOGP) rule

- The LOGP is a consensus rule for combining several source-specific posterior probabilities with considering weights for controlling the relative influence of each data source.

$$L_c((\mathbf{x}_i)_1,\ldots,(\mathbf{x}_i)_q)=\prod_{m=1}^{q} p_m(y_i=c\,|\,(\mathbf{x}_i)_m)^{\alpha_m}$$

- Using LOGP rule and considering the parameters associated with the classifiers, we can calculate the final posterior probabilities as:

$$p_{LOGP}(y_i=c\,|\,(\mathbf{x}_i)_1,\ldots,(\mathbf{x}_i)_q,\boldsymbol{\omega}_1,\ldots,\boldsymbol{\omega}_q,\alpha_1,\ldots,\alpha_q)=\frac{\prod_{m=1}^{q} p_m(y_i=c\,|\,(\mathbf{x}_i)_m,\boldsymbol{\omega}_m)^{\alpha_m}}{\sum_{c=1}^{K}\prod_{m=1}^{q} p_m(y_i=c\,|\,(\mathbf{x}_i)_m,\boldsymbol{\omega}_m)^{\alpha_m}}$$

J. Benediktsson, J. Sveinsson, and P. Swain, "Hybrid consensus theoretic classification," IEEE Transactions on Geoscience and Remote Sensing, vol. 35, no. 4, pp. 833–843, Jul. 1997.

Combination of LOGP and MLRsub

- Using MLRsub to model the posterior probabilities of each feature vector and LOGP rule for combining the source-specific posterior probabilities , we can now obtain:

$$p_{LOGP}(y_i = c \mid (\mathbf{x}_i)_1, \ldots, (\mathbf{x}_i)_q, \boldsymbol{\omega}_1, \ldots, \boldsymbol{\omega}_q, \alpha_1, \ldots, \alpha_q) = \frac{\exp\left(\sum_{m=1}^{q} \alpha_m \boldsymbol{\omega}_m^{(c)^T} \varphi((\mathbf{x}_i)_m)\right)}{\sum_{c=1}^{K} \exp\left(\sum_{m=1}^{q} \alpha_m \boldsymbol{\omega}_m^{(c)^T} \varphi((\mathbf{x}_i)_m)\right)}$$

- Combining the regressors and the weight parameters into a new set of regressors:

$$\tilde{\boldsymbol{\omega}}_m^{(c)} = \alpha_m \boldsymbol{\omega}_m^{(c)}$$

$$p_{LOGP}(y_i = c \mid (\mathbf{x}_i)_1, \ldots, (\mathbf{x}_i)_q, \tilde{\boldsymbol{\omega}}_1, \ldots, \tilde{\boldsymbol{\omega}}_q) = \frac{\exp\left(\sum_{m=1}^{q} \tilde{\boldsymbol{\omega}}_m^{(c)^T} \varphi((\mathbf{x}_i)_m)\right)}{\sum_{c=1}^{K} \exp\left(\sum_{m=1}^{q} \tilde{\boldsymbol{\omega}}_m^{(c)^T} \varphi((\mathbf{x}_i)_m)\right)}$$

University of Houston data

- Comprises 349x1905 pixels and 144 spectral bands between 0.38 and 1.05 microns.
- Spatial resolution of 2.5 meters, with 2832 training samples and 12197 test samples.

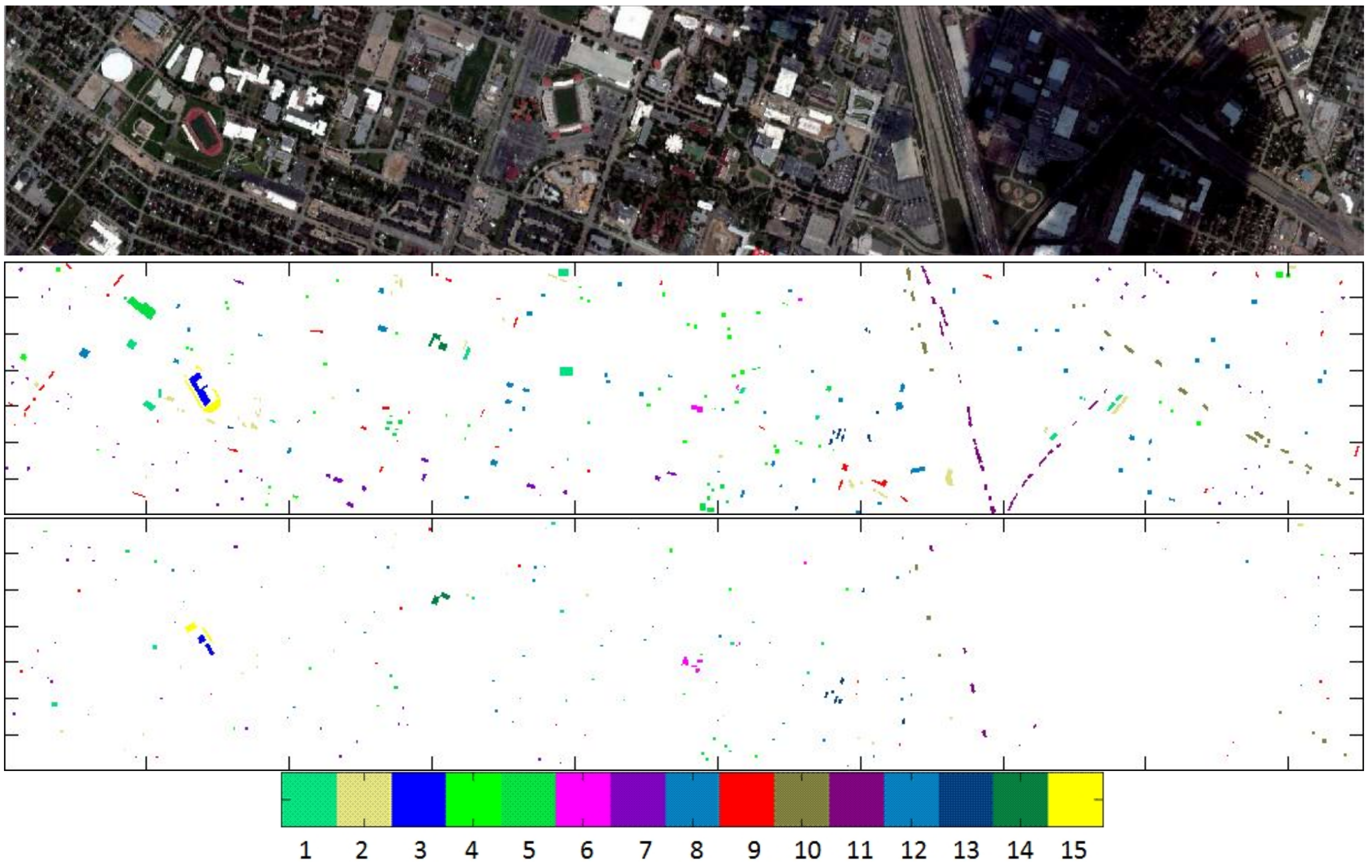

False color composition

Reference data

Training data

Labels color: 1-Healthy grass, 2-Stressed grass, 3-Synthetic grass, 4-Trees, 5-Soil, 6-Water, 7-Residential, 8-Commercial, 9-Road, 10-Highway, 11-Railway, 12-Parking Lot 1, 13-Parking Lot 2, 14-Tennis Court, 15-Running Track

University of Houston data

- University of Houston data set consists of a hyperspectral image and a LiDAR derived DSM, both at the same spatial resolution (2.5m).

False color composition

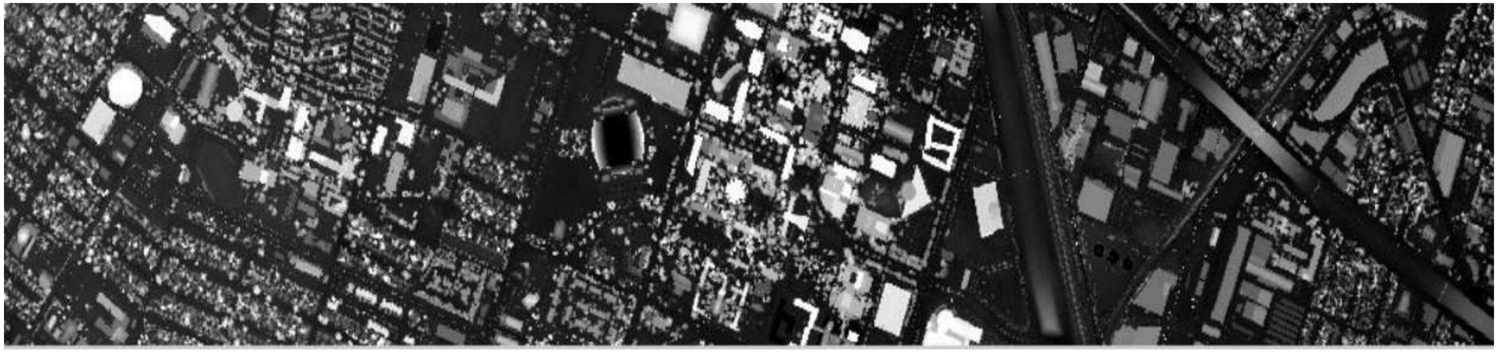

LiDAR derived DSM

Classification results

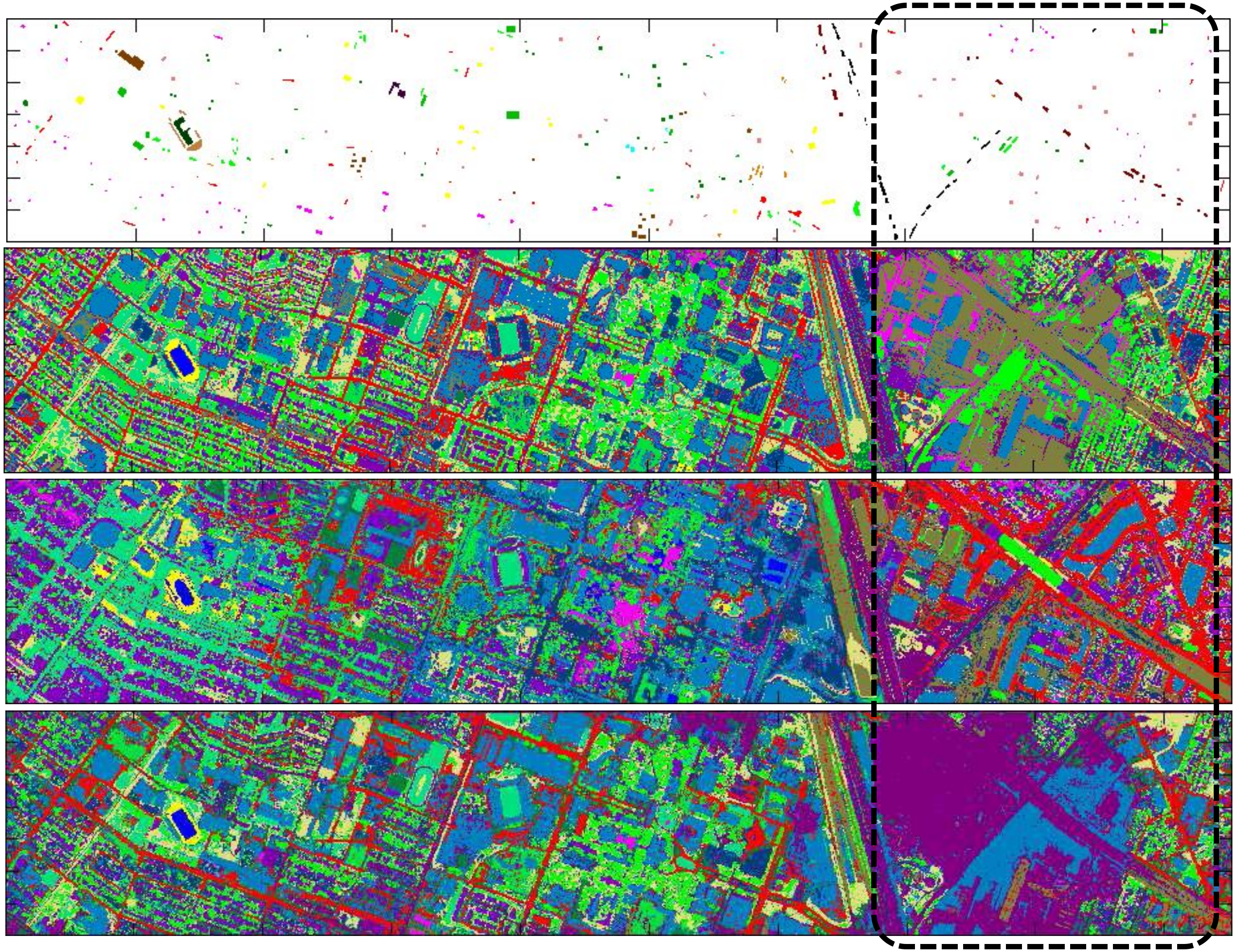

Ground Truth

MLRsub using Xh (79.60%)

MLRsub using AP(XL) (58.08%)

MLRsub using EMAP(Xh) (74.53%)

Classification results

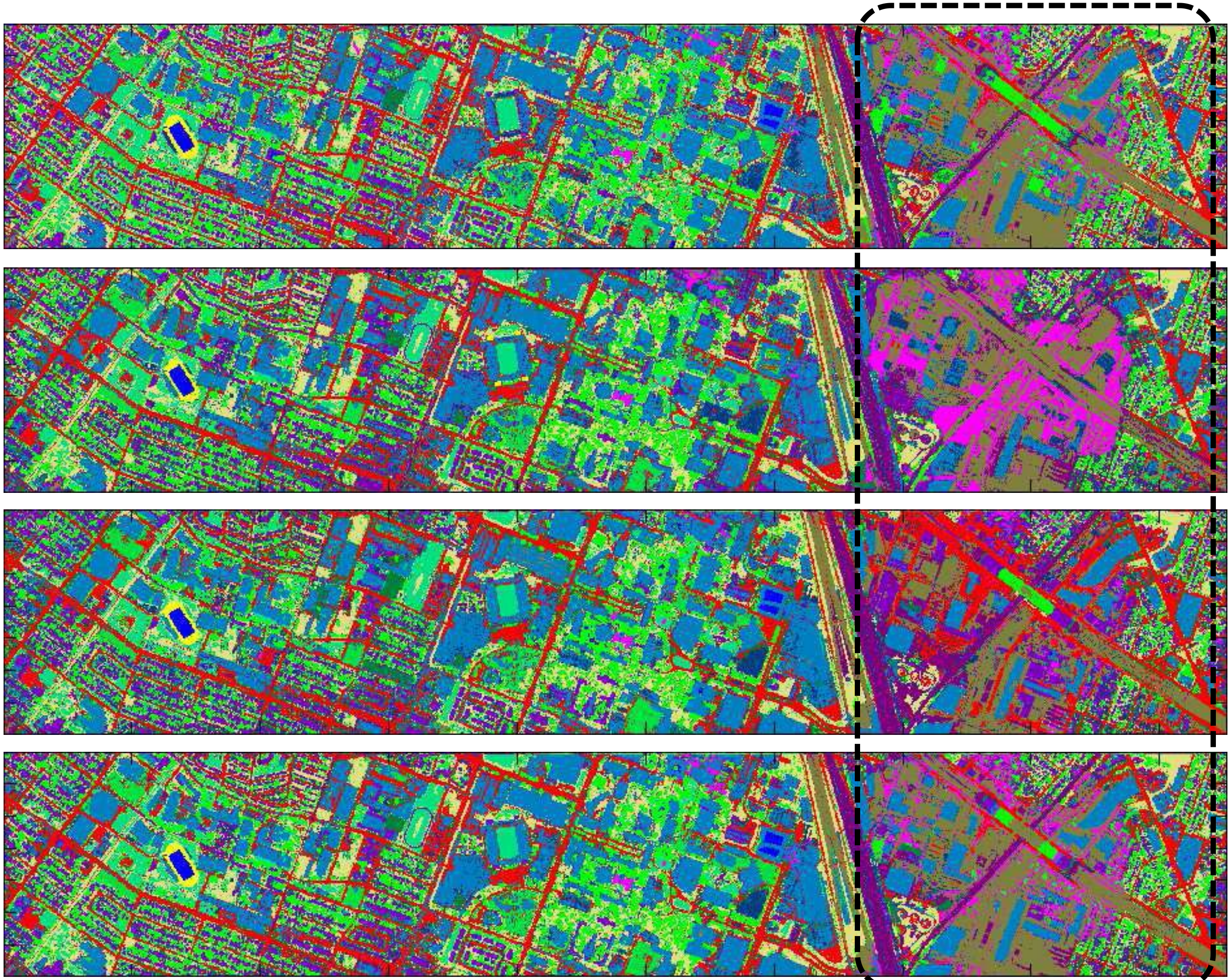

MLRsub using Xh+AP(XL) (87.91%)

MLRsub using Xh+EMAP(Xh) (84.40%)

MLRsub using AP(XL)+EMAP(Xh) (86.86%)

MLRsub using Xh+AP(XL)+EMAP(Xh) (90.65%)

Outline

1. Introduction
2. Combining local and global probabilities
3. MLRsub algorithm based on class-indexed subspaces
4. MLRsub algorithm based on union of subspaces
5. Probabilistic relaxation
6. Fusion of hyperspectral and LiDAR data
7. Conclusions and future research lines

Conclusions

Probabilistic Relaxation

Subspace Concept

Future research lines

- The integration of techniques for spectral unmixing and classification.
- Developing an unified framework based on union of subspaces.
- Computationally efficient implementations of the new techniques developed in this thesis.

Publications

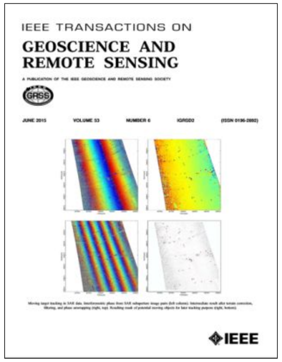

1. M. Khodadadzadeh, J. Li, A. Plaza, H. Ghassemian, J. M. Bioucas-Dias and X. Li, "Spectral-Spatial Classification of Hyperspectral Data Using Local and Global Probabilities for Mixed Pixel Characterization," IEEE Transactions on Geoscience and Remote Sensing, vol. 52, no. 10, pp. 6298-6314, October 2014 [JCR(2014)=3.514].

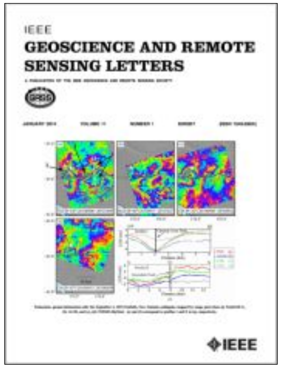

2. M. Khodadadzadeh, J. Li, A. Plaza and J. M. Bioucas-Dias, "A Subspace Based Multinomial Logistic Regression for Hyperspectral Image Classification," IEEE Geoscience and Remote Sensing Letters, vol. 11 no. 12, pp. 2105-2109, December 2014 [JCR(2014)=2.095].

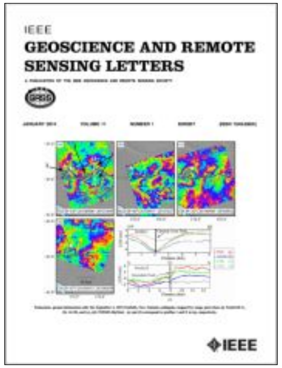

3. L. Gao, J. Li, M. Khodadadzadeh, A. Plaza, B. Zhang, Z. He, and H. Yan., "Subspace-Based Support Vector Machines for Hyperspectral Image Classification," IEEE Geoscience and Remote Sensing Letters, vol. 12 no. 2, pp. 349-353, February 2015 [JCR(2014)=2.095].

Publications

4. M. Khodadadzadeh, J. Li, S. Prasad and A. Plaza, "Fusion of Hyperspectral and LiDAR Remote Sensing Data Using Multiple Feature Learning," IEEE Journal of Selected Topics in Applied Earth Observations and Remote Sensing, accepted for publication, 2015 [JCR(2014)=3.026].

5. J. Li, M. Khodadadzadeh, A. Plaza, X. Jia and J. M. Bioucas-Dias, "A Discontinuity Preserving Relaxation scheme for Spectral-Spatial Hyperspectral Image Classification," IEEE Journal of Selected Topics in Applied Earth Observations and Remote Sensing, accepted for publication subject to minor revisions, 2015 [JCR(2014)=3.026].

- 10 international conference papers including IEEE IGARSS, WHISPERS and IEEE JURSE.

Research stay

University: Instituto de Telecomunicações, Instituto Superior Técnico, Universidade de Lisboa

Advisor: Jose M. Bioucas Dias

Academic year: 2013-2014

Department of Technology of Computers and Communications
Escuela Politécnica de Cáceres, University of Extremadura

Thank You

Ph.D. Thesis:

New Probabilistic Classification Techniques for Hyperspectral Images

Author: Mahdi Khodadadzadeh

Advisors: Antonio Plaza Miguel
Jun Li